World Journal of Stem Cells

Submit a Manuscript: https://www.f6publishing.com

World J Stem Cells 2024 December 26; 16(12): 1022-1046

DOI: 10.4252/wjsc.v16.i12.1022

ISSN 1948-0210 (online)

ORIGINAL ARTICLE

Basic Study

Exosomes derived from microRNA-540-3p overexpressing mesenchymal stem cells promote immune tolerance *via* the CD74/nuclear factor-kappaB pathway in cardiac allograft

Ji-Gang He, Xin-Xin Wu, Si Li, Dan Yan, Gao-Peng Xiao, Fu-Gang Mao

Specialty type: Cell and tissue engineering

Provenance and peer review: Unsolicited article; Externally peer reviewed.

Peer-review model: Single blind

Peer-review report's classification

Scientific Quality: Grade B, Grade C, Grade C, Grade C

Novelty: Grade B, Grade C, Grade C

Creativity or Innovation: Grade B, Grade B, Grade C

Scientific Significance: Grade B, Grade B, Grade B

P-Reviewer: Amin A; Capone D; Li SC

Received: May 14, 2024

Revised: September 16, 2024

Accepted: November 12, 2024

Published online: December 26, 2024

Processing time: 212 Days and 18.8 Hours

Ji-Gang He, Si Li, Department of Cardiovascular Surgery, The First People's Hospital of Yunnan Province, Kunming 650032, Yunnan Province, China

Xin-Xin Wu, Yunnan University of Traditional Chinese Medicine, Kunming 650500, Yunnan Province, China

Dan Yan, Department of Medical Intensive Care Unit, The First People's Hospital of Yunnan Province, Kunming 650032, Yunnan Province, China

Gao-Peng Xiao, Department of Anaesthesia, The First People's Hospital of Yunnan Province, Kunming 650032, Yunnan Province, China

Fu-Gang Mao, Department of Ultrasonic, The First People's Hospital of Yunnan Province, Kunming 650032, Yunnan Province, China

Corresponding author: Fu-Gang Mao, MD, Professor, Department of Ultrasonic, The First People's Hospital of Yunnan Province, No. 157 Jinbi Road, Kunming 650032, Yunnan Province, China. maofugang666@163.com

Abstract

BACKGROUND

Heart transplantation is a crucial intervention for severe heart failure, yet the challenge of organ rejection is significant. Bone marrow mesenchymal stem cells (BMSCs) and their exosomes have demonstrated potential in modulating T cells, dendtitic cells (DCs), and cytokines to achieve immunomodulatory effects. DCs, as key antigen-presenting cells, play a critical role in shaping immune responses by influencing T-cell activation and cytokine production. Through this modulation, BMSCs and their exosomes enhance graft tolerance and prolonging survival.

AIM

To explore the immunomodulatory effects of exosomes derived from BMSCs overexpressing microRNA-540-3p (miR-540-3p) on cardiac allograft tolerance, focusing on how these exosomes modulating DCs and T cells activity through the CD74/nuclear factor-kappaB (NF-κB) pathway.

METHODS

Rat models were used to assess the impact of miR-540-3p-enhanced exosomes on immune tolerance in cardiac allografts. MiR-540-3p expression was manipulated in BMSCs, and derived exosomes were collected and administered to the rat models post-heart transplantation. The study monitored expression levels of major histocompatibility complex II, CD80, CD86, and CD274 in DCs, and quantified $CD4^+$ and $CD8^+$ T cells, T regulatory cells, and cytokine profiles.

RESULTS

Exosomes from miR-540-3p-overexpressing BMSCs lead to reduced expression of immune activation markers CD74 and NF-κB p65 in DCs and T cells. Rats treated with these exosomes showed decreased inflammation and improved cardiac function, indicated by lower levels of pro-inflammatory cytokines (interleukin-1β, interferon-γ) and higher levels of anti-inflammatory cytokines (interleukin-10, transforming growth factor β1). Additionally, miR-540-3p skewed the profiles of DCs and T cells towards immune tolerance, increasing the ratio of T regulatory cells and shifting cytokine secretion to favor graft acceptance.

CONCLUSION

Exosomes derived from BMSCs overexpressing miR-540-3p significantly enhance immune tolerance and prolong cardiac allograft survival by modulating the CD74/NF-κB pathway, which regulates activities of DCs and T cells. These findings highlight a promising therapeutic strategy to improve heart transplantation outcomes and potentially reduce the need for prolonged immunosuppression.

Key Words: Bone marrow mesenchymal stem cells; Exosomes; MicroRNA-540-3p; Cardiac allograft; Immune tolerance

Core Tip: This study explores the innovative use of exosomes from bone marrow mesenchymal stem cells overexpressing microRNA-540-3p to promote immune tolerance in heart transplantation. Demonstrating a significant modulation of the CD74/nuclear factor-kappaB pathway, these exosomes enhance graft survival and function by altering dendritic and T cell responses. Our findings suggest a promising therapeutic strategy that reduces the need for prolonged immunosuppression, offering a substantial advancement in transplant medicine. This approach underscores the potential of targeted exosomal therapies in improving outcomes for heart transplant patients.

Citation: He JG, Wu XX, Li S, Yan D, Xiao GP, Mao FG. Exosomes derived from microRNA-540-3p overexpressing mesenchymal stem cells promote immune tolerance *via* the CD74/nuclear factor-kappaB pathway in cardiac allograft. *World J Stem Cells* 2024; 16(12): 1022-1046

URL: https://www.wjgnet.com/1948-0210/full/v16/i12/1022.htm

DOI: https://dx.doi.org/10.4252/wjsc.v16.i12.1022

INTRODUCTION

Heart failure constitutes a significant global public health concern, affecting at least 26 million individuals worldwide, with its prevalence showing an upward trajectory[1]. Currently, heart transplantation remains the primary therapeutic approach for patients with advanced heart failure[2]. However, rejection of transplanted organs by the immune system poses a formidable challenge, and prolonged use of immunosuppressive drugs to secure graft acceptance often results in adverse reactions and toxicity[3]. Attaining immune tolerance in transplanted organs without extended immunosuppression is a crucial objective in transplantation science. Therefore, the development of strategies to prevent immune rejection is important for heart transplantation.

Dendritic cells (DCs) and T cells are key factors in allograft rejection after transplantation. DCs are professional antigen-presenting cells (APCs) that guide T-cell activation and are responsible for eliminating self-reactive T-cells that evade thymic elimination, thereby contributing to the prevention of autoimmune responses[4]. Research has indicated that the co-administration of DC and T regulatory cells (Treg) promotes allograft survival in heart transplantation. Recently, exosomes derived from DCs were found to modulate the adaptive immune response to pathogens and tumors [5]. T cell activation is a necessary step for allograft rejection because the limitation of DCs migration or proliferation could prevent immune rejection in heart transplantation. Thus, environmental molecules are responsible for the fate of immune cells and contribute to the development of DCs and immune rejection[6].

Studies have indicated that mesenchymal stem cells (MSCs) possess the ability to regulate the immune system by influencing macrophage polarization[7], suppressing DC maturation[8], prolonging neutrophil viability[9], inhibiting natural killer cell proliferation and cytotoxicity[10], suppressing T effector cell proliferation, promoting Treg proliferation [11,12], and suppressing B cell proliferation and activation in a T cell-dependent manner[13]. MSCs exert their immunomodulatory effects through either cell-cell interactions or paracrine activities[14,15], involving the release of transforming growth factor beta (TGFβ), interferon-gamma (IFN-γ), prostaglandin E2, interleukin (IL)-10, tumor necrosis

factor-alpha (TNF-α), and indoleamine 2,3-dioxygenase (IDO) through a cytokine-dependent mechanism[16]. The potential of MSCs as valuable resources for cell therapy has also been demonstrated. Their remarkable ability to reduce inflammation and suppress the immune system makes them highly desirable for treating graft-*versus*-host diseases and preventing graft rejection[17]. However, inadequate viability of transplanted MSCs hampers the efficacy of MSC treatment[18].

Exosomes are lipid vesicles released by various cell types including MSCs, DCs[19], B cells[20], and T cells[21]. They typically have diameters of 40-100 nm[22]. Following secretion, exosomes can be internalized by either nearby or remote cells, resulting in the transfer of molecular cargo that can affect the physiology and function of the receiving cell[23]. Recent studies have shown that exosomes derived from MSCs have a crucial impact on controlling the biological activities of MSCs, thereby enhancing their therapeutic capabilities[24,25], and could potentially function as a substitute for the transplantation of MSCs in cell therapy[26-30]. In addition, they modulate the immune system and promote tissue repair[23,31,32]. MSC-derived exosomes have also demonstrated the ability to inhibit T cell activation and contribute to the maintenance of immune homeostasis[33]. Exosomes possess various benefits over their parental cells, such as reduced immunogenicity and the absence of tumor formation risks[24]. It has been suggested that exosomes can potentially be used for cell-free treatment instead of MSC transplantation. In terms of immune modulation, exosomes present a significantly lower risk profile compared to the direct genetic modification of immune cells. One possibility is to use MSC-derived exosomes for the treatment of cardiovascular and cerebrovascular diseases[34,35], graft-*versus*-host diseases [36-38], and neurodegenerative diseases[39].

Although exosomes have therapeutic potential, their stability and effectiveness remain a concern when considering their clinical applications. Consequently, exosomes have been generated from MSCs that have undergone preconditioning or epigenetic modifications[24]. Our previous study showed that exosomes derived from IDO-expressing rat bone marrow MSCs (BMSCs) could regulate the activity of DCs and T cells *in vitro* and *in vivo*, as specified by cell markers and cytokines, as well as promote survival and immune tolerance of recipient hearts[40,41]. Bioinformatics data revealed that microRNA-540-3p (miR-540-3p) exhibited the greatest increase in expression among the miRNAs found in exosomes derived from BMSCs expressing IDO[41]. Furthermore, we discovered that miR-540-3p, which was significantly upregulated along with another upregulated protein, immunoregulatory four-and-a-half LIM domain protein 1, negatively impacted Janus kinase 3, an immune stimulator, and hindered the activation of protein kinase B (Akt). Consequently, this inhibition impedes the development and operation of DCs[41]. Because miR-540-3p is significantly upregulated in exosomes secreted by IDO-expressing BMSCs[41], we hypothesized that miR-540-3p may play a role in IDO-mediated MSC-derived exosome-mediated immunomodulation.

CD74, also known as the invariant chain of major histocompatibility complex (MHC) class II, functions as a chaperone for MHC II and plays a crucial role in the MHC II-mediated antigen presentation pathway[42-44]. Previous studies have demonstrated that lipopolysaccharide (LPS) stimulates an increase in CD74 expression in B cells. Furthermore, inhibition of the nuclear factor-kappaB (NF-κB) pathway has been shown to reduce LPS-induced expression of CD74[45], indicating that CD74 may exert its activity through NF-κB activation. CD74 is widely expressed in various immune cells, including B cells, activated T cells, DCs, monocytes/macrophages, and Langerhans cells[46]. It has also been implicated in numerous immune-related disorders, including autoimmune diseases[44]. NF-κB, a versatile transcription factor found in nearly all mammalian cells, plays a role in processes such as inflammation, immune response, cell survival, proliferation, and differentiation[47]. NF-κB activation is observed in transplanted solid organs, and specifically inhibiting NF-κB can enhance graft survival with reduced adverse effects compared with broad immunosuppressive treatments in specific cell populations[48]. However, further investigation is required to explore the potential collaboration between CD74 and NF-κB in allograft rejection and to understand the associated mechanisms. In the present study, we investigated the role of miR-540-3p in immunomodulation and cardiac allograft tolerance by two approaches: (1) We established miR-540-3p-knock-in and -knock-out rat models; and (2) Wild-type (WT) rats were injected with exosomes derived from miR-540-3p-overexpressing BMSCs.

MATERIALS AND METHODS

Animals

Healthy male specific-pathogen-free Sprague Dawley (SD) and Wistar rats, aged 4-6 weeks and weighing 200-250 g, were procured from Hunan SJA Laboratory Animal Co., Ltd. (Hunan, China). MiR-540-3p-knock-in and miR-540-3p-knock-out rats were obtained from Cyagen Biosciences Inc. (Guangzhou, China). All animal experiments adhered to the ARRIVE principles, were conducted with the assistance of Yunan Labreal Biotech Ltd., and were approved by the Animal Care and Use Committee of Yunan Labreal Biotech Ltd. (Certificate: No. SL20220510).

Establishment of BMSC culture

SD rat BMSCs were extracted from the femur and tibia following a previously described protocol[41]. Briefly, the rats were anesthetized with a single intravenous injection of sodium pentobarbital (200 mg/kg) before euthanasia *via* cervical dislocation. The femur and tibia were collected and immersed in 75% ethanol for 2 minutes and then in 0.9% normal saline. The bone marrow was flushed, the femur and tibia were chopped into cubes, and the liquid was transferred to a sterilized tube. Following centrifugation at 1500 × *g* for 10 minutes, the cell pellet was resuspended in bone marrow MSC growth medium (Cyagen Biosciences, Sunnyvale, CA, United States) supplemented with 10% fetal bovine serum (Gibco, Thermo Fisher Scientific, United States). The cells were incubated at 37 °C with 5% CO_2 for 72 hours, and the medium was changed every three days. Cells at passage 7 were used for subsequent experiments. Expressed (CD73, CD90, CD44 and

CD29) and unexpressed (CD11b, CD34 and CD45) markers of MSC were analyzed by flow cytometry (Supplementary Figure 1).

MiRNA transfection

BMSCs overexpressing or downregulating miR-540-3p were generated *via* transfection. Cells in the exponential growth phase were inoculated at 2 × 10^5 cells/well in 24-well plates, cultured overnight, and then transfected with miR-540-3p-mimic (50 nM), miR-540-3p-inhibitor (100 nM), and miRNA negative control (NC) (50 nM) using riboFECT™ CP Reagent and Buffer (RiboBio, Guangzhou, China) as per the manufacturer's instructions. Briefly, 1.25 μL of the miR was diluted with 30 μL riboFECT™ CP buffer. The diluent was mixed with 3 μL riboFECT™ CP reagent and incubated at room temperature for 10 minutes. The riboFECT CP-miR mixture was added to the cells along with the cell culture medium and incubated at 37 °C with 5% CO_2 for 48 hours. This procedure was also applied to DCs and T cell transfection experiments.

Construction of BMSCs overexpressing IDO

BMSCs overexpressing IDO ($BMSC^{IDO}$) were generated using a previously established lentiviral transduction method[40]. In summary, the rat *IDO1* gene was inserted into the lentiviral vector GV308, and the resulting recombinant plasmids were introduced into *Escherichia coli* DH5α. HEK293 cells were co-transfected with the recombinant plasmids pHelper 1.0, and pHelper 2.0, to package the lentivirus. After 48 hours of cell culture, the collected supernatant was used to infect BMSCs.

Extraction of BMSCs-derived exosomes

Exosomes were extracted using the ExoQuick technique, as described previously[41]. Briefly, following a 48-hour culture period, the cells were centrifuged at 300 × *g* for 15 minutes at 4 °C to obtain the supernatant. The supernatant was further centrifuged at 15000 × *g* for 30 minutes at 4 °C and the resulting supernatant was filtered through a 0.2-μm filter. The filtrate was then centrifuged at 120000 × *g* for 70 minutes at 4 °C and exosomes were harvested using an ExoQuick-TC kit (System Biosciences, Mountain View, California, United States).

Preparation and culture of DCs

DCs from SD rats were obtained using a previously described method[41]. Briefly, after sedation, the aorta was isolated, and blood samples were collected. Blood was combined with erythrocyte lysis buffer (Solarbio Co., Ltd., Beijing, China) and incubated on ice for 15 minutes with intermittent vortexing. Lymphocytes were obtained using Lymphocyte Separation Medium (Prathipati *et al*[28]) (Solarbio Co., Ltd., Beijing, China). After resuspending the cells in erythrocyte lysis buffer, the mixture was centrifuged at 450 × *g* for 10 minutes at 4 °C. The cell pellet was resuspended in RPMI 1640 medium containing 10% fetal bovine serum, 20 ng/mL granulocyte-macrophage colony-stimulating factor, and 10 ng/mL IL-4. Cells were cultured for 10 days, and DCs were isolated using anti-rat DC (OX62) MicroBeads (Miltenyi) according to the manufacturer's instructions. DCs were identified by detecting OX62-positive cells based on their morphology using an electron microscope.

Preparation and culture of T cells

SD rat T cells were obtained using methods outlined in a previous study[40]. Briefly, spleens were aseptically harvested, minced, and processed into single-cell suspensions. After treatment with erythrocyte lysis solution, the mixture was cooled on ice for 15 minutes with intermittent agitation. Cell collection was achieved by centrifugation at 450 × *g* for 10 minutes at 4 °C. For cell sorting, the suspension was centrifuged at 300 × *g* for 10 minutes and resuspended in MACS buffer. The cell suspension was incubated with anti-DC (OX62) microbeads at 4 °C for 15 minutes. After washing, centrifugation, and resuspension, the cells were passed through a column, following the manufacturer's instructions. The resulting T cells were observed under a phase-contrast microscope.

Real-time reverse transcriptase-polymerase chain reaction

Total RNA was extracted using TRIzol reagent according to the manufacturer's instructions (Thermo Scientific, Waltham, MA, United States). RNA concentration was determined using a Nanodrop (ND-1000). cDNA was synthesized using the Bulge-Loop miRNA qRT-PCR Starter Kit (C10211-1; Ribobio, Guangzhou, China). Primers were designed and synthesized by RiboBio (Guangzhou, China). Quantitative real-time polymerase chain reaction (qPCR) was performed using 2 × SYBR Green Master Mix (5 μL), RT product (1 μL), Bulge-Loop™ miRNA Forward Primer (5 μmol/L, 0.4 μL), Bulge-Loop™ miRNA Reverse Primer (5 μmol/L, 0.4 μL), ROX (0.2 μL) in a total reaction volume of 10 μL. U6 was used as the internal reference, and the relative expression level of miR-540-3p was determined using the $2^{-\Delta\Delta Ct}$ method. This experiment was repeated six times. These procedures are also applicable to animal experiments. The primer for rno-miR-540-3p was shown as: Forward 5'-AGAGGCGACCGGGCCA-3', reverse: 5'-AGTGCAGGGTCCGAGGTATT-3'.

Co-culture of cells and BMSCs-derived exosomes

DCs, T cells, and DCs + T cells (DCs:T cells = 1:1) were co-cultured with the following BMSC-derived exosomes: (1) Exosomes from untreated BMSCs (BMSC exosome); (2) Exosomes from BMSCs transfected with miR-NC ($BMSC^{NC}$ exosome); (3) Exosomes from BMSCs transfected with miR-540-3p-mimic ($BMSC^{miR\text{-}540\text{-}3p\text{-}mimic}$ exosome); (4) Exosomes from BMSCs transfected with miR-540-3p-inhibitor ($BMSC^{miR\text{-}540\text{-}3p\text{-}inhibitor}$ exosome); and (5) Exosomes from BMSCs infected with IDO-containing lentivirus ($BMSC^{IDO}$ exosome). Untreated cells served as cell-only controls. All co-culture groups, except the cell-only control group, were also treated with LPS (5 μg/mL) to induce an immune response. The concentration of

exosomes from corresponding BMSCs was adjusted to 5 μg/mL before addition to cells (all in the number of 10^7). The co-culture was incubated at 37 °C with 5% CO_2 for 72 hours before subsequent experiments.

Western blot analysis

Western blot analysis was used to determine the expression levels of CD74 and NF-κB p65. Cells (DCs and T cells) underwent lysis with RIPA buffer containing phosphatase and protease inhibitors (Beyotime Biotechnology, China) for 30 minutes at 4 °C. Protein concentration was determined using the BCA assay following the manufacturer's instructions (Beyotime Biotechnology, China). Proteins were separated using 10% sodium dodecyl sulfate-polyacrylamide gel electrophoresis and transferred onto a polyvinylidene fluoride membrane (Millipore) using the wet transfer method. After blocking with 5% bovine serum albumin (Solarbio Co., Ltd, Beijing, China), the membrane was incubated overnight at 4 °C with anti-CD74 polyclonal antibody (1:1000 dilution; ThermoFisher PA5-22113), anti-NFκB p65 monoclonal antibody (1:200 dilution; ThermoFisher 436700), and anti-GAPDH monoclonal antibody (1:1000 dilution; Abmart M20006). Subsequently, the membranes were incubated with horseradish peroxidase-conjugated secondary antibodies (1:2000 dilution; Cat. No. 7074 or 7076, Cell Signal Technology) for 2 hours at room temperature. Signals were visualized using an enhanced chemiluminescence reagent (Solarbio Co., Ltd., Beijing, China). Band intensities were semi-quantitatively analyzed using ImageJ software, with GAPDH bands serving as loading controls to normalize the gray values. Each experiment was repeated six times. This procedure is also applicable in animal experiments.

Flow cytometry analysis

Flow cytometry was used to analyze DCs and T-cell surface markers. After 72 hours of co-culture, cells were harvested and incubated with the following antibodies: Phycoerythrin-conjugated anti-CD80 (eBioscience™, Thermo Fisher Scientific, Cat. No. 12-0800-82), Alexa Flμor® 488-conjugated anti-CD86 (Abcam, Cat. No. ab256270), allophycocyanin-conjugated anti-MHC II (anti-HLA-DR) (Cat. No. bs-1198R-APC), and fluorescein isothiocyanate (FITC)-conjugated anti-CD274 (Cat. No. bs-4941R-FITC), and FITC-conjugated anti-CD3 (eBioscience, Thermo Fisher Scientific, Cat. No. 11-0030-82), FITC-conjugated anti-CD4 (eBioscience™, Thermo Fisher Scientific, Cat. No. 11-0040-82), allophycocyanin-conjugated anti-CD8 (eBioscience™, Thermo Fisher Scientific, Cat. No. 17-0084-82), and allophycocyanin -conjugated anti-CD25 (eBioscience™, Thermo Fisher Scientific, Cat. No. 17-0390-82). The stained cells were analyzed using a flow cytometer (ACEA NovoCyte™ 2060R, United States). Each experiment was repeated six times. This procedure is also applicable in animal experiments.

ELISA analysis

Cell culture supernatants or serum samples from animal experiments were collected to determine cytokine levels. The samples were assayed using commercially available rat enzyme-linked immunosorbent assay kits (Mlbio, China) for IL-1β (Cat. No. ml037361) and IFN-γ (Cat. No. ml064291), IL-10 (Cat. No. ml037371) and TGFβ1 (Cat. No. ml002856). The optical density was measured using a microplate reader (SpectraMax 190, Molecular Devices Corporation, United States) at 450 nm immediately after the addition of the stop solution. Each experiment was repeated six times.

Prediction of miRNA target and dual-luciferase

The binding sites of CD74 with miR-540-3p were predicted using TargetScan ver_7.2 (https://www.targetscan.org/mmu_72/). Gene Ontology annotation and Kyoto Encyclopedia of Genes and Genomes pathway enrichment analyses were conducted using the clusterProfiler R package to ensure a false discovery rate of less than 0.05. Gene Ontology annotations encompassed terms related to biological processes, molecular functions, and cellular components. WT and mutant plasmids were constructed and cloned into the pRL-REPORT plasmid. HEK 293T cells were cultured in 24-well plates at a density of 2×10^5 cells/well. Subsequently, the cells were transfected with pRL-REPORT plasmids, miR-540-3p mimics, or their respective NCs using Lipofectamine 2000. The luciferase activities of Renilla and fireflies were determined using a Luciferase Reporter Assay Kit (Promega, China). Relative luciferase activity was determined by normalizing the results to the deviation of firefly/Renilla luciferase activity.

Co-immunoprecipitation analysis

At 36 hours after transfection, DCs and T cells were harvested and lysed in pre-cooled RIPA buffer for 30 minutes at 4 °C. The cell lysate was centrifuged at 12000 × *g* for 30 minutes at 4 °C to collect the supernatant. Next, rabbit anti-rat NF-κB p65 immunoglobulin G (CST Cat. No. 8242) or rabbit anti-rat immunoglobulin G (control) was added to the supernatant, and the mixture was incubated overnight at 4 °C. The protein A/G beads (Sc0102, Elabscience), washed with pre-cooled RIPA buffer, were then added to the mixture, incubated at 4 °C for 2 hours, centrifuged at 8000 × *g* for 30 seconds, and the pellet was harvested for western blotting to detect CD74.

Heterotopic heart transplantation

Heterotopic heart transplantation was performed as previously described[40]. Donors (Wistar rats) and recipients (SD rats, miR-540-3p knock-in rats, or miR-540-3p knock-out rats) underwent surgery at 7-9 weeks of age, with a body weight of 250-300 g. Random numbers for the animal groups were generated using the Rand function in Microsoft Excel. The rats were anesthetized with an intravenous injection of sodium pentobarbital (30 mg/kg). After anticoagulation (50 U/L heparin), cardiac arrest was induced by infusing 5 mL of cold saline solution into the heart. The cardiac grafts were excised and transplanted into the recipient abdomen. The signs of hind leg paralysis, tail stiffness, or bruising of the toenail tips indicated failure. Animal caregivers and model operators were unaware of the grouping to ensure consistent care, monitoring, and handling. Rats undergoing heart transplantation were injected with normal saline (1 mL) or

exosomes (2 mL, 5 μg/mL) *via* the tail vein three days post-surgery. The exosome types included BMSC, $BMSC^{NC}$, $BMSC^{miR\text{-}540\text{-}3p\text{-}mimic}$, $BMSC^{miR\text{-}540\text{-}3p\text{-}inhibitor}$, and $BMSC^{IDO}$ exosomes. Rats that did not undergo transplantation were administered normal saline (1 mL) as a control. For statistical independence, six rats were selected from each group, in total 52 Wistar rat donors and 58 SD rats (43 WT SD rats, seven miR-540-3p knock-in rats, and eight miR-540-3p knock-out rats). Two rats experienced intervention hemorrhage during heterotopic heart transplantation, and two died within 12 hours post-model construction. The main causes of model mortality are bleeding, infection, or postoperative rejection, and heart failure[49,50]. The animals were kept under standard conditions, and all experiments were performed in compliance with the principles of laboratory animal care (NIH publication No. 86-23, revised 1985). All animal experiments were performed using the platform of Yunan Labreal Biotech Ltd., Co., and conducted by the co-author Jigang He in accordance with the ARRIVE principles and were approved by the Animal Care and Use Committee of Yunan Labreal Biotech Ltd., Co. (Approval number: No. SL20220510). The primary goal of this study was to collect foundational experimental data to support future complex designs; thus, a small sample size is warranted for statistical independence. After seven days, the animals were euthanized through over-anesthesia (intravenous injection of sodium pentobarbital (200 mg/kg), followed by cervical dislocation. The endpoint was set as when an animal was unable to eat or drink without anesthesia or sedation, was unable to stand for up to 24 hours, or could stand only with extreme reluctance. Heart samples and blood were fixed for histopathological analysis or rapidly frozen using liquid nitrogen and preserved at -80 °C for later examination.

Echocardiographic assessments of ventricular function

Heart function was assessed using a color Doppler echocardiography instrument (PHILIPS EPIQ 7C; Philips, Best, Netherlands) 72 hours after heart transplantation[41]. Left ventricular (LV) parameters were obtained from 2-dimensional images and M-mode interrogation in the long-axis view. The LV ejection fraction (B-mode) and fractional shortening (M-mode) were determined using previously described formulas[40] and measured over three cardiac cycles.

Histological and morphological examination

For histological and morphological examinations, heart grafts were obtained 72 hours after transplantation. The harvested heart tissues underwent fixation in 4% neutral buffered paraformaldehyde for 24 hours, paraffin embedding, and subsequent sectioning at a thickness of 5 μm. Hematoxylin and eosin staining was performed, and the LV myocardium was examined under a light microscope (Olympus CKX41, Olympus, Tokyo, Japan).

Statistical analysis

Data were analyzed using GraphPad Prism 8 (GraphPad Software, La Jolla, California, United States). Results are presented as the mean ± SD. Group differences were evaluated using one-way analysis of variance (ANOVA), followed by a post-hoc Bonferroni test. Statistical significance was set at $P < 0.05$.

RESULTS

Overexpression of miR-540-3p in DCs or T cells enhanced the immune tolerance

In our previous study, we identified the top 20 up- and down-regulated miRNAs in IDO-overexpressed BMSC exosomes compared with BMSC exosomes were selected using the criteria set at $|\text{Log2 fold change (FC)}| \geq 1.5$ and P value ≤ 0.05. Among these miRNAs, ten immune-related candidates[41] (rno-miR-540-3p, rno-miR-1188-5p, rno-miR-434-3p, rno-miR-431, rno-miR-200a-5p, rno-miR-136-5p, rno-miR-375-3p, rno-miR-466b-5p, rno-miR-25-5p, and rno-miR-338-5p) were selected based on their gene symbols (Figure 1A, Table 1). Additionally, we performed qPCR to detect immune-related miRNAs in exosomes. The qPCR results indicated that rno-miR-466b-5p, rno-miR-25-5p, and rno-miR-338-5p were downregulated, whereas rno-miR-540-3p, rno-miR-1188-5p, rno-miR-434-3p, rno-miR-431, rno-miR-200a-5p, rno-miR-136-5p, and rno-miR-375-3p were upregulated in IDO-overexpressing exosomes compared to exosomes derived from BMSCs and BMSCs transfected with NC plasmids (Figure 1B). Notably, miR-540-3p showed the most highly upregulated expression in the qPCR analysis. Furthermore, as demonstrated in our previous study[41], DC and T cell states are modulated by IDO-overexpressing BMSC exosomes, prompting further investigation into how miR-540-3p overexpression or inhibition specifically affects immune responses in DCs and T cells.

To explore this, DCs and T cells were transfected with the miR-540-3p mimic, miR-540-3p inhibitor, and their corresponding NCs, followed by treatment with LPS, a potent activator of immune cells including B cells, monocytes, macrophages, and other LPS-reactive cells. The expression of miR-540-3p was assessed using qPCR at 48, 72, and 96 hours post-transfection. In both DCs and T cells, the miR-540-3p-mimic group exhibited significantly higher expression than the control and NC groups at all three time points, with peak expression observed at 72 hours. Conversely, the miR-540-3p inhibitor group showed a significant decrease in expression 72 and 96 hours post-transfection (Figure 1C). Subsequent experiments were conducted 72 hours after plasmid transfection. Flow cytometry analysis showed that the expression of surface markers, including CD80, CD86, MHC II, and CD274, was significantly increased in DC stimulated with LPS for 72 hours (Figure 1D-G). In addition, DCs transfected with the miR-540-3p inhibitor showed increased expression of MHC II (Figure 1D), CD80 (Figure 1E), and CD86 (Figure 1F), but decreased expression of CD274 (Figure 1G). Conversely, transfection with the miR-540-3p mimic produced the opposite effect, reducing the expression of MHC II, CD80, and CD86 while increasing CD274 levels.

Table 1 Immune-related microRNA in top 20 up regulated microRNAs

miRNA ID	Log2FC	miRBase ID	Up/down	Gene symbol
rno-miR-540-3p	7.17	MIMAT0003174	Up	Jak3
rno-miR-1188-5p	6.244	MIMAT0017854	Up	Cd28
rno-miR-434-3p	5.002	MIMAT0005315	Up	Aicda
rno-miR-431	4.411	MIMAT0001626	Up	Icos
rno-miR-200a-5p	4.149	MIMAT0017151	Up	RT1-N2
rno-miR-136-5p	2.921	MIMAT0000842	Up	Cd80
rno-miR-375-3p	2.84	MIMAT0005307	Up	Tshr
rno-miR-466b-5p	-1.713	MIMAT0005278	Down	Cxcl12
rno-miR-25-5p	-1.786	MIMAT0004713	Down	Cd4
rno-miR-338-5p	-1.936	MIMAT0004646	Down	Rag2

miRNA: MicroRNA; FC: Fold change; JAK3: Janus kinase 3.

The supernatant of cell culture was collected to examine cytokine secretion. In DC cells, LPS treatment significantly increased pro-inflammatory cytokine levels (IL-1β and IFN-γ) as well as anti-inflammatory cytokines (IL-10 and TGFβ1). After miR-540-3p inhibitor transfection, pro-inflammatory cytokine levels were increased, but anti-inflammatory cytokine levels were significantly decreased in LPS exposed to DCs co-cultured with T cells (Figure 1H-K). Conversely, transfection with the miR-540-3p mimic produced the opposite effect, decreasing pro-inflammatory cytokines while increasing anti-inflammatory cytokines. These results indicate that miR-540-3p regulates the expression of surface markers in DCs and influences the cytokine levels secreted by DCs co-cultured with T cells under LPS exposure.

Subsequently, we examined the effect of miR-540-3p overexpression on cytokine expression in T cells and T cells co-cultured with DCs using the same approach. Similarly, the miR-540-3p-mimic group exhibited peak expression at 72 hours post-transfection (Figure 2A). Following LPS stimulation, the ratios of $CD4^+$ T cells, $CD8^+$ T cells, and Tregs were significantly higher than those of the normal T cells. Transfection with the miR-540-3p mimic reduced the ratios of $CD4^+$ and $CD8^+$ T cells while increasing the ratio of Tregs. Conversely, transfection with the miR-540-3p inhibitor increased the ratios of $CD4^+$ and $CD8^+$ T cells while decreasing the ratio of Tregs (Figure 2B-D, Supplementary Figure 2). The secretion of IL-1β, IFN-γ, IL-10, and TGFβ1 was increased in LPS-stimulated T cells compared to normal T cells without LPS stimulation. However, transfection with the miR-540-3p mimic resulted in a decrease in IL-1β and IFN-γ concentrations in T cells and T cells co-cultured with DCs, accompanied by an increase in IL-10 and TGFβ1 concentrations. Conversely, transfection with the miR-540-3p inhibitor increased IL-1β and IFN-γ levels while decreasing IL-10 and TGFβ1 concentrations secreted by T cells and T cells co-cultured with DCs (Figure 2E-H). These results indicate that miR-540-3p regulates the ratios of T cell subgroups and influences the cytokine levels secreted by T cells and T cells co-cultured with DCs.

Co-culture with BMSC$^{miR\text{-}540\text{-}3p\ mimic}$ exosomes enhanced the immune tolerance in DCs and T cells

Based on the findings that miR-540-3p modulates immune responses in DCs and T cells and that environmental molecular signals influence immune cell development and function, we further investigated whether BMSC-derived exosomes carrying miR-540-3p could promote immune tolerance in DCs and T cells. Transmission electron microscopy showed that BMSC exosomes exhibited a theatre-like structure and a size of approximately 50-100 nm, with a bilayer structure featuring clearly defined membrane boundaries (Figure 3A). Nanosight analysis revealed particle sizes ranging from 133.4 to 226.5 nm, displaying irregular Brownian motion and a concentration of 3.8×10^9 particles/mL (Figure 3B). Our data demonstrated that BMSC transfected with miR-540-3p produced exosomes carrying miR-540-3p, with a maximum at 72 hours post-plasmid transfection (Figure 3C). Exosomes from BMSCs at 72 hours post-transfection were used in subsequent experiments. The expression of miR-540-3p in DCs and T cells was assessed after co-culturing with exosomes. The expression of miR-540-3p was significantly higher in DCs and T cells co-cultured with BMSC exosomes, and it further increased after co-culture with BMSC$^{miR\text{-}540\text{-}3p\text{-}mimic}$ exosomes or BMSC^{IDO} exosomes compared to that in the BMSC exosome group. In contrast, expression decreased after co-culture with BMSC$^{miR\text{-}540\text{-}3p\text{-}inhibitor}$ exosomes compared to DCs and T cells co-cultured with BMSC exosomes (Figure 3D and E).

The positivity rate for MHC II, CD80, and CD86 was decreased (Figure 4A-C), whereas the positivity rate of CD274 (Figure 4D) was increased after co-culture with BMSC$^{miR\text{-}540\text{-}3p\text{-}mimic}$ exosomes or BMSC^{IDO} exosomes compared to those in the BMSC exosome group. Conversely, the positivity rate of MHC II, CD80, and CD86 was increased after co-culture with BMSC$^{miR\text{-}540\text{-}3p\text{-}inhibitor}$ exosomes (Figure 4A-C, Supplementary Figure 3). The concentrations of the pro-inflammatory cytokines IL-1β and IFN-γ, as well as the anti-inflammatory cytokines IL-10 and TGFβ1, secreted by DCs were also investigated (Figure 4E-H). The concentrations of IL-1β, IFN-γ, IL-10, and TGFβ1 increased compared with normal DCs after LPS stimulation. After co-culture with BMSC exosomes, the concentrations of IL-1β and IFN-γ decreased, while IL-10 and TGFβ1 increased. Furthermore, the concentrations of IL-1β and IFN-γ further decreased, and the concentrations of IL-10

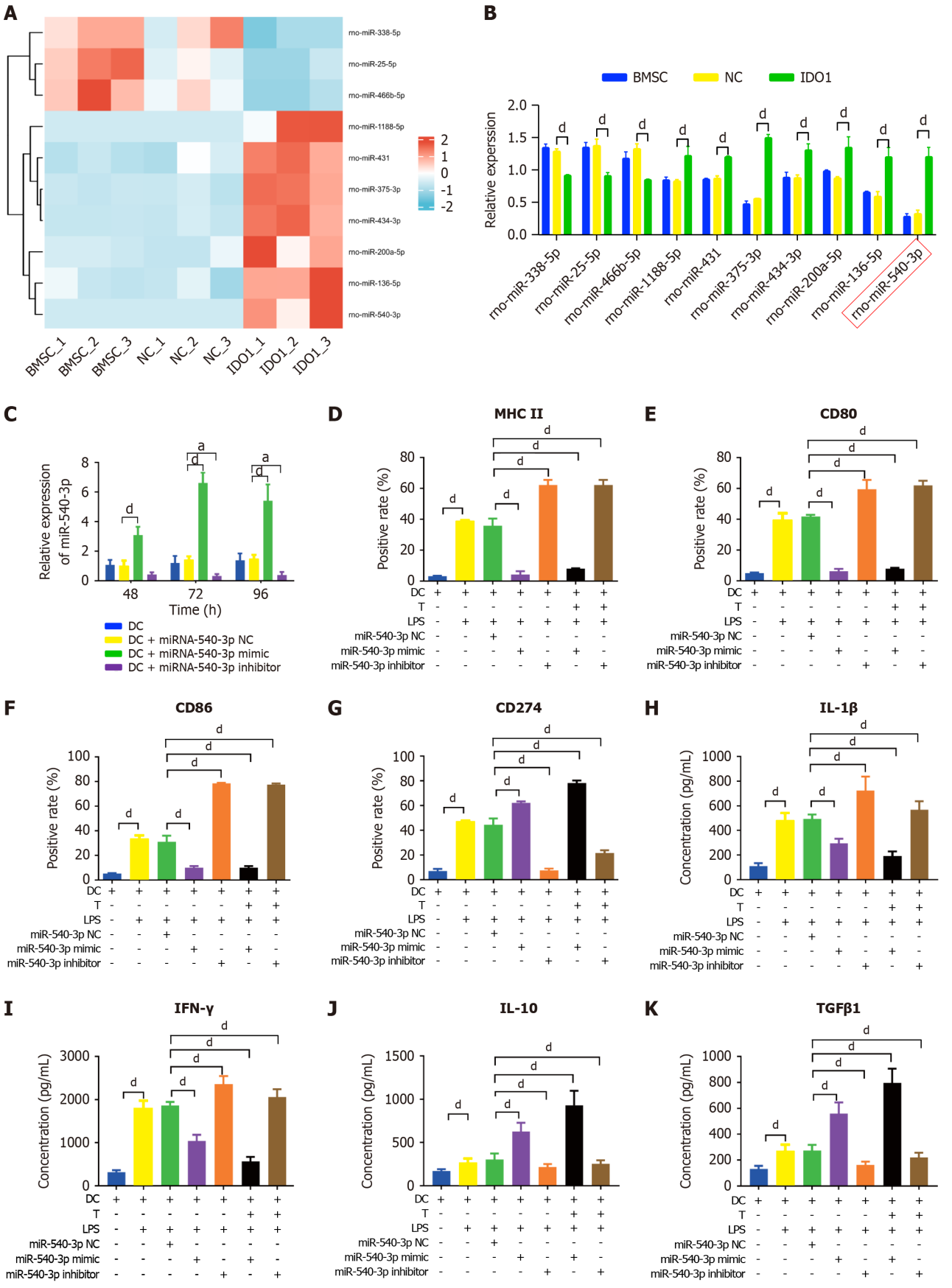

Figure 1 Overexpression of microRNA-540-3p in dendritic cells modulates surface markers and cytokine production. A: Ten immune-related microRNAs (miRNAs) in indoleamine 2,3-dioxygenase-overexpressing bone marrow mesenchymal stem cell exosomes compared to those in bone marrow mesenchymal stem cell exosomes; B: Quantification of immune-related miRNA expression by quantitative real-time polymerase chain reaction; C: Expression of miR-540-3p in dendritic cells (DCs) at 48, 72, and 96 hours after transfection; D-G: Flow cytometry analysis of the positive rate of cell surface markers in DCs (major

histocompatibility complex II, CD80, CD86, CD274) and DCs after co-culture with T cells for 72 hours; H-K: Enzyme-linked immunosorbent assay-based quantitative analysis of cytokine production (interleukin-1β, interferon-γ, interleukin-10, transforming growth factor β1) in DCs and DCs after co-culture with T cells for 72 hours. $^{a}P < 0.05$, $^{d}P < 0.0001$. BMSC: Bone marrow mesenchymal stem cell; NC: Negative control; IDO: Indoleamine 2,3-dioxygenase; DC: Dendritic cell; LPS: Lipopolysaccharide; IL: Interleukin; TGF: Transforming growth factor; IFN: Interferon.

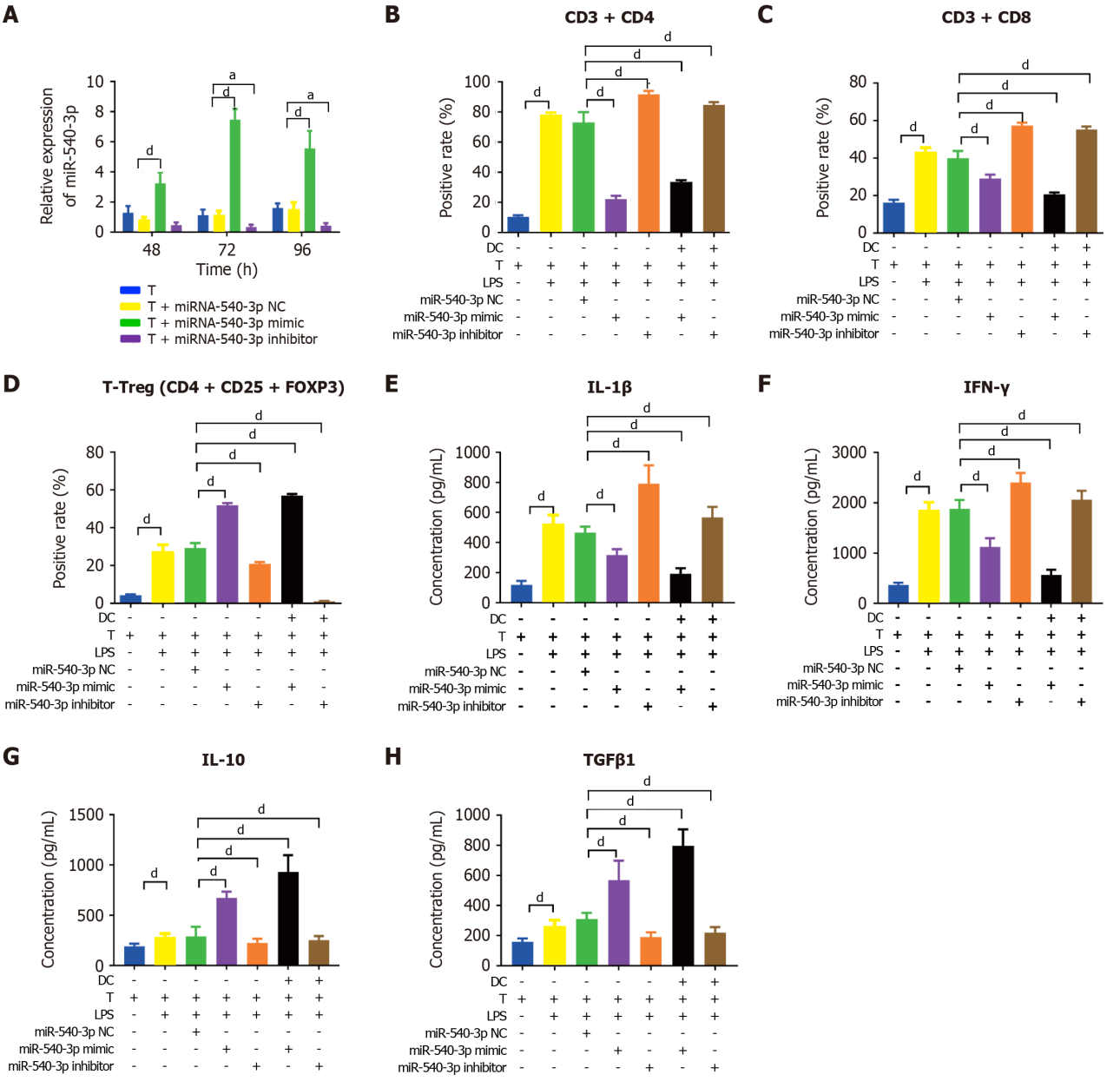

Figure 2 Overexpression of microRNA-540-3p in T cells modulates cell subtypes and cytokine production. A: Expression of microRNA-540-3p in T cells at 48, 72, and 96 hours post-plasmid transfection; B-D: Flow cytometry analysis of the positive rate of T cells ($CD4^+$ T, $CD8^+$ T, and T regulatory cell) and T cells after co-culture with dendritic cells for 72 hours; E-H: Enzyme-linked immunosorbent assay-based quantitative analysis of cytokine production (interleukin-1β, interferon-γ, interleukin-10, and transforming growth factor β1) in T cells and T cells after co-culture with dendritic cells for 72 hours. $^{a}P < 0.05$, $^{d}P < 0.0001$. NC: Negative control; LPS: Lipopolysaccharide; IL: Interleukin; TGF: Transforming growth factor; IFN: Interferon.

and TGFβ1 further increased after co-culture with $BMSC^{miR\text{-}540\text{-}3p\text{-}mimic}$ exosomes and $BMSC^{IDO}$ exosomes compared to the BMSC exosome group. Conversely, the concentrations of IL-1β and IFN-γ increased, and the concentrations of IL-10 and TGFβ1 decreased after co-culture with $BMSC^{miR\text{-}540\text{-}3p\text{-}inhibitor}$ exosomes compared with the BMSC exosome group. These results indicate that miR-540-3p affects the DC phenotype and mediates pro-/anti-inflammatory cytokine secretion in DC exposed to LPS.

The ratios of $CD4^+$ T cells, $CD8^+$ T cells, and Tregs were assessed. After LPS stimulation, the ratios of $CD4^+$ and $CD8^+$ T cells increased, whereas the ratio of Tregs decreased compared to those in the LPS-negative group; the ratios of $CD4^+$ and $CD8^+$ T cells further decreased, whereas the ratio of Tregs further increased after treatment with $BMSC^{miR\text{-}540\text{-}3p\text{-}mimic}$ exosomes and $BMSC^{IDO}$ exosomes. Conversely, the ratios of $CD4^+$ T cells and $CD8^+$ T cells increased, while the ratio of

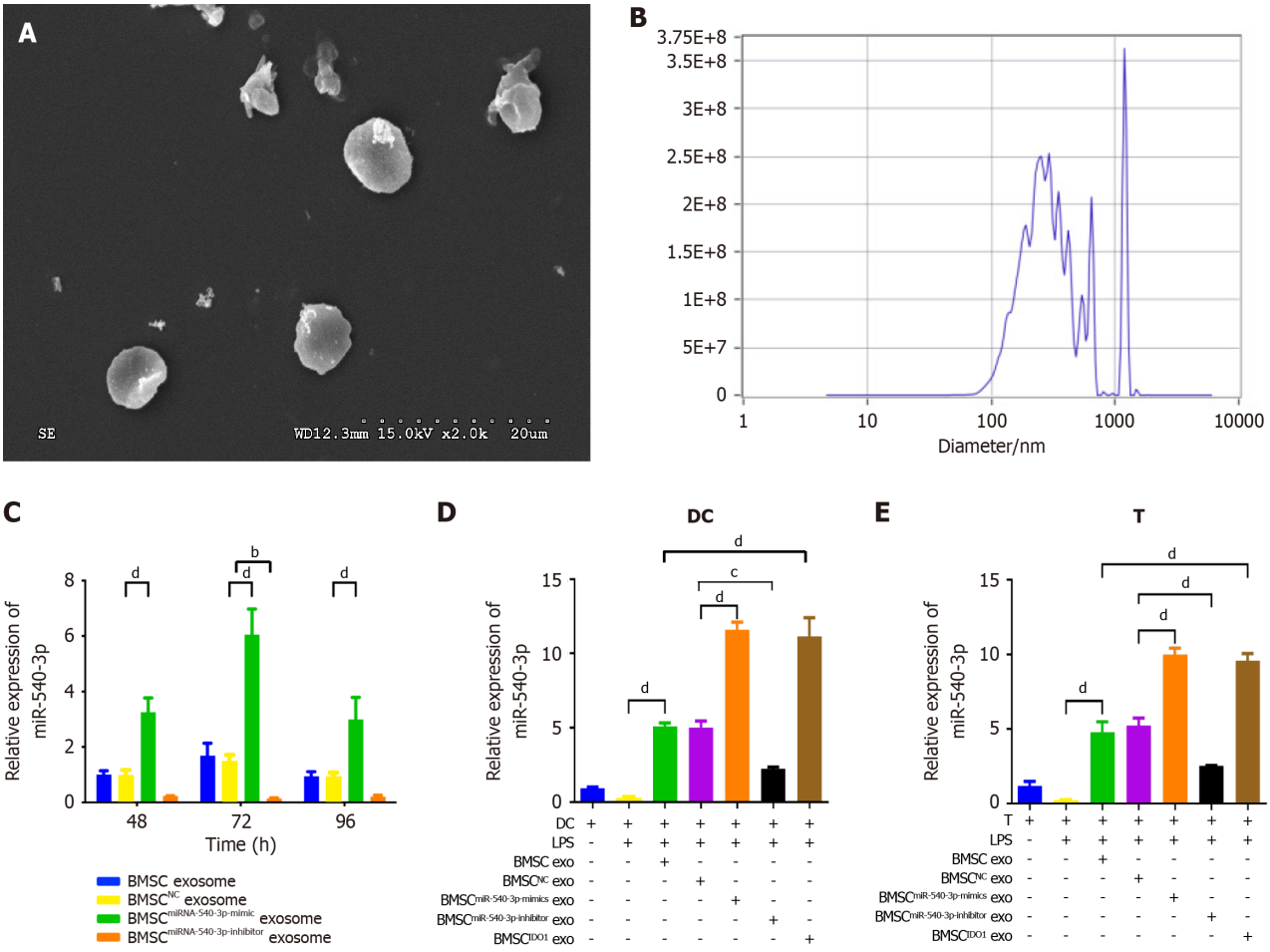

Figure 3 Production and characterization of bone marrow mesenchymal stem cell$^{miR\text{-}540\text{-}3p\text{-}mimic}$ exosomes. A: Transmission electron microscopy image of isolated exosomes; B: Nanosight analysis for exosome size and concentration; C: Expression of microRNA-540-3p (miR-540-3p) in bone marrow mesenchymal stem cell-derived exosomes at 48, 72, and 96 hours after plasmid transfection; D: Expression of miR-540-3p in dendritic cells; E: Expression of miR-540-3p in T cells. $^{b}P < 0.01$, $^{c}P < 0.001$, $^{d}P < 0.0001$. BMSC: Bone marrow mesenchymal stem cell; IDO: Indoleamine 2,3-dioxygenase; DC: Dendritic cell; LPS: Lipopolysaccharide; exo: Exosomes.

Tregs decreased after treatment with BMSC$^{miR\text{-}540\text{-}3p\text{-}inhibitor}$ exosomes compared to those in the BMSC exosome group (Figure 5A-C, Supplementary Figure 3). The extracellular level of the secreted pro-inflammatory cytokines IL-1β and IFN-γ, as well as the anti-inflammatory cytokines IL-10 and TGFβ1 in T cell supernatant, all increased after LPS stimulation compared with that without LPS treatment (Figure 5D-G). After co-culture with BMSC exosomes, the levels of IL-1β and IFN-γ secreted by T cells decreased, while IL-10 and TGFβ1 increased. Moreover, the concentrations of IL-1β and IFN-γ further decreased, and the concentrations of IL-10 and TGFβ1 further increased after co-culture with BMSC$^{miR\text{-}540\text{-}3p\text{-}mimic}$ exosomes and BMSC^{IDO} exosomes compared to the BMSC exosome group. In contrast, the secretion of IL-1β and IFN-γ in T cells culture increased, and the levels of IL-10 and TGFβ1 decreased after co-culture with BMSC$^{miR\text{-}540\text{-}3p\text{-}inhibitor}$ exosomes compared with the BMSC exosome group. Therefore, exosomes from miR-540-3p-overexpressing BMSC suppressed inflammation and promoted anti-inflammatory effects in LPS-stimulated T-cells exposed to LPS.

To mimic the conditions of immune tolerance, we co-cultured DCs with T cells and stimulated them with LPS and found that the levels of DCs surface markers, including MHC II, CD80, CD86, and CD274, were significantly increased. The positivity rate of DC markers and the proportion of T cells increased after LPS stimulation. After co-culture with BMSC exosomes, the positivity rates of MHC II, CD80, and CD86, as well as the ratio of $CD4^+$ T cells to $CD8^+$ T cells, decreased. In contrast, the positivity rate of CD274 and the ratio of Tregs increased, and these effects were further observed after co-culture with BMSC$^{miR\text{-}540\text{-}3p\text{-}mimic}$ exosomes and BMSC^{IDO} exosomes, compared to the BMSC exosome group. The positivity rate of MHC II and the ratio of $CD4^+$ T cells to $CD8^+$ T cells increased, whereas the ratio of Tregs decreased after co-culture with BMSC$^{miR\text{-}540\text{-}3p\text{-}inhibitor}$ exosomes (Figure 6A-G, Supplementary Figure 3). Moreover, the expression of secreted IL-1β, IFN-γ, as well as IL-10 and TGFβ1, in culture supernatant from co-cultured DCs and T cells were also investigated (Figure 6H-K). The concentrations of IL-1β, IFN-γ, IL-10, and TGFβ1 increased after LPS stimulation. After co-culture with BMSC exosomes, the concentrations of IL-1β and IFN-γ decreased, whereas those of IL-10 and TGFβ1 increased. The concentrations of IL-1β and IFN-γ further decreased, and the concentrations of IL-10 and TGFβ1 further increased after co-culture with BMSC$^{miR\text{-}540\text{-}3p\text{-}mimic}$ exosomes and BMSC^{IDO} exosomes compared with the BMSC exosome group. Conversely, the concentrations of IL-1β and IFN-γ increased, and the concentrations of IL-10 and TGFβ1 decreased after co-culture with BMSC$^{miR\text{-}540\text{-}3p\text{-}inhibitor}$ exosomes compared with the BMSC exosome group. These results demonstrate that co-culture with BMSC$^{miR\text{-}540\text{-}3p\text{-}mimic}$ exosomes enhances immune tolerance in DCs and T cells.

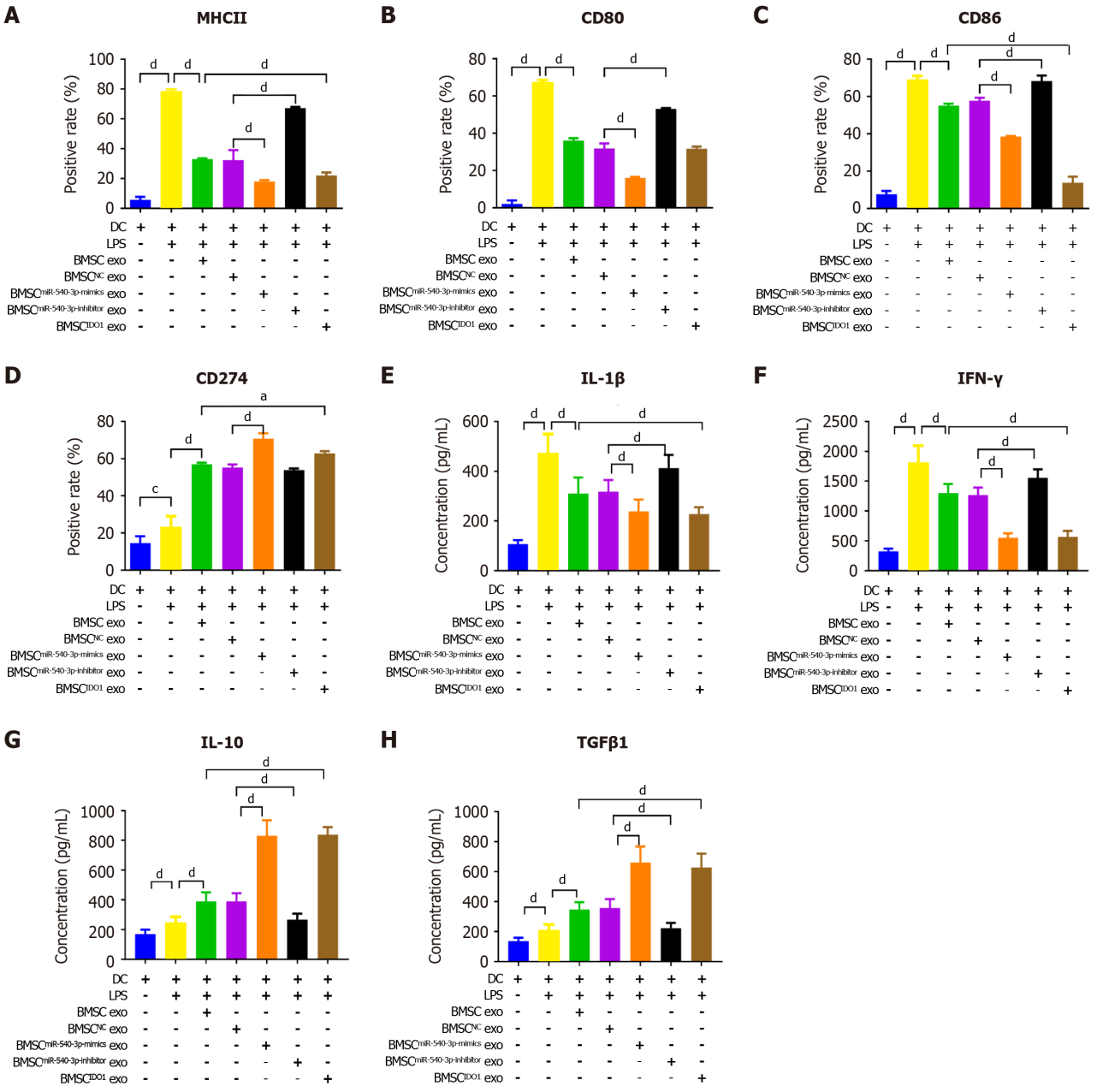

Figure 4 Bone marrow mesenchymal stem cell$^{miR\text{-}540\text{-}3p\text{-}mimic}$ exosomes reduces immune resistance in dendritic cells. A-D: Flow cytometry analysis of the positive rate of cell surface markers in dendritic cells (major histocompatibility complex II, CD80, CD86, and CD274) for 72 hours; E-H: Enzyme-linked immunosorbent assay-based quantitative analysis of cytokine production (interleukin-1β, interferon-γ, interleukin-10, transforming growth factor β1) in dendritic cells. $^{a}P < 0.05$, $^{d}P < 0.0001$. MHC: Major histocompatibility complex; BMSC: Bone marrow mesenchymal stem cell; IDO: Indoleamine 2,3-dioxygenase; DC: Dendritic cell; LPS: Lipopolysaccharide; exo: Exosomes; IL: Interleukin; TGF: Transforming growth factor; IFN: Interferon.

Co-culture with BMSC$^{miR\text{-}540\text{-}3p\text{-}mimic}$ exosomes decreased the expression of CD74 and NF-κB p65 in DCs and T cells

MiRNAs exert their functions by binding to the 3′ untranslated region of target mRNAs, leading to the downregulation of their expression. Target genes of miR-540-3p were predicted using TargetScan (http://www.targetscan.org/vert_72/), and subsequent Gene Ontology and Kyoto Encyclopedia of Genes and Genomes enrichment analyses of the target genes were conducted (Supplementary Tables 1 and 2). The results revealed that the target genes of miR-540-3p were principally enriched in the regulation of neuronal projection development, epithelial tube morphogenesis, and homophilic cell adhesion *via* plasma membrane adhesion molecules (Figure 7A).

CD74 is essential for MHC class II antigen presentation and, by activating extracellular signal-regulated kinase-1/2 and phosphoinositide 3-kinase/protein kinase B/SRC signaling pathways, modulates the functions of macrophages, dendritic cells, T cells, and B cells, thereby orchestrating immune responses and playing a key role in allogeneic transplantation (https://reurl.cc/34Grrj). Accordingly, we aim to investigate the potential involvement of CD74 in the immunomodulatory effects of miR-540-3p. The binding of CD74 to miR-540-3p was predicted, and a dual-luciferase assay was performed. Co-transfection of miR-540-3p mimics and WT CD74 plasmids resulted in decreased relative luciferase activity compared to cells co-transfected with NC mimics and WT CD74 plasmids. Conversely, when miR-540-3p mimics or NC mimics were co-transfected with mutant CD74 plasmids, there was no significant change in the relative luciferase

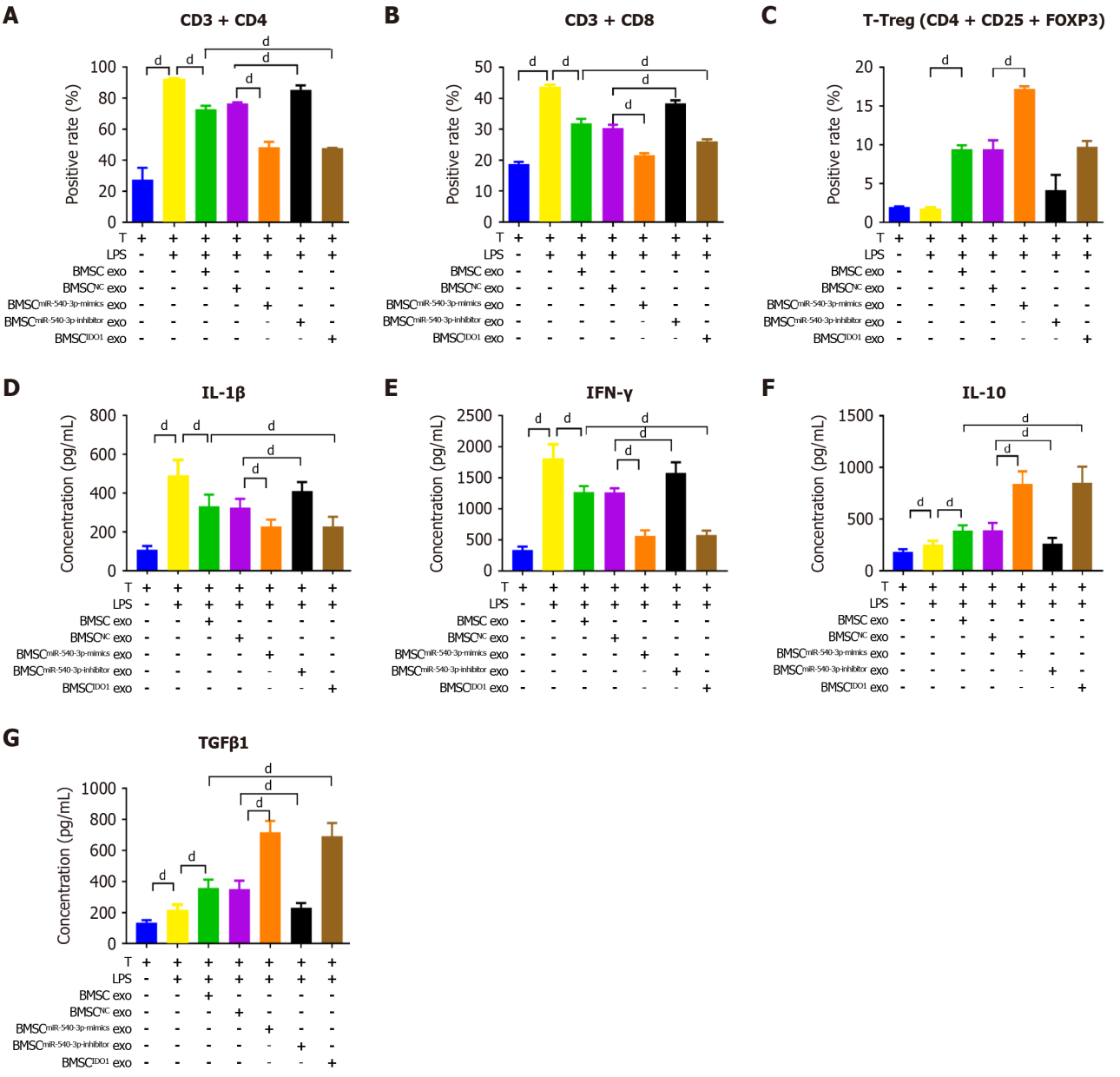

Figure 5 Bone marrow mesenchymal stem cell$^{miR\text{-}540\text{-}3p\text{-}mimic}$ exosomes reduces immune resistance in T cells. A-C: Flow cytometry analysis of the positive rate of $CD4^+$ T cells, $CD8^+$ T cells, and regulatory T cells for 72 hours; D-G: Enzyme-linked immunosorbent assay-based quantitative analysis of cytokine production (interleukin-1β, interferon-γ, interleukin-10, and transforming growth factor β1) in T cells. $^dP < 0.0001$. BMSC: Bone marrow mesenchymal stem cell; LPS: Lipopolysaccharide; exo: Exosomes; IL: Interleukin; TGF: Transforming growth factor; IFN: Interferon.

activity (Figure 7B). These findings indicate that CD74 is a target of miR-540-3p.

Additionally, the transcription factor NF-κB p65 is considered a downstream target of CD74. The interaction between CD74 and NF-κB p65 was verified through a co-immunoprecipitation experiment after transfection of CD74 and NF-κB p65 in DCs and T cells. These results demonstrated that CD74 co-precipitated with NF-κB p65. Upon LPS stimulation of DCs or T cells, co-precipitation was more pronounced, and this effect decreased when cells were co-cultured with BMSC exosmes and further decreased when cells were co-cultured with BMSC$^{miR\text{-}540\text{-}3p\text{-}mimic}$ exosomes (Figure 7C and D).

Subsequently, the expression levels of CD74 and NF-κB p65 were determined using western blotting in different co-culture scenarios involving DCs, T cells, or DCs and T cells with various BMSC-derived exosomes. After co-culture with BMSC exosomes, the expression levels of CD74 and NF-κB p65 were significantly lower in BMSC$^{miR\text{-}540\text{-}3p\text{-}mimic}$ exosomes and BMSC^{IDO} exosomes co-cultured with DCs, T cells, or extracted DCs and T cells. In contrast, the expression levels of CD74 and NF-κB p65 were significantly higher in BMSC$^{miR\text{-}540\text{-}3p\text{-}inhibitor}$ exosomes compared to BMSC exosome-co-cultured cells (Figure 7E-P). Furthermore, the expression levels of CD74 and NF-κB p65 were determined in DCs and T cells transfected with the miR-540-3p mimic, miR-540-3p inhibitor, or the corresponding NC. Following LPS stimulation, the expression of CD74 and NF-κB p65 increased in DCs and T cells. At 72 hours post-transfection, the expression levels of CD74 and NF-κB p65 in DCs or T cells transfected with miR-540-3p-mimic were significantly lower, while the expression was higher in DCs or T cells transfected with miR-540-3p-inhibitor or extracted DCs or T cells after cell co-culture (Figure 7Q-V). Building on these findings, we extended our investigation to an *in vivo* ectopic heart transplantation model

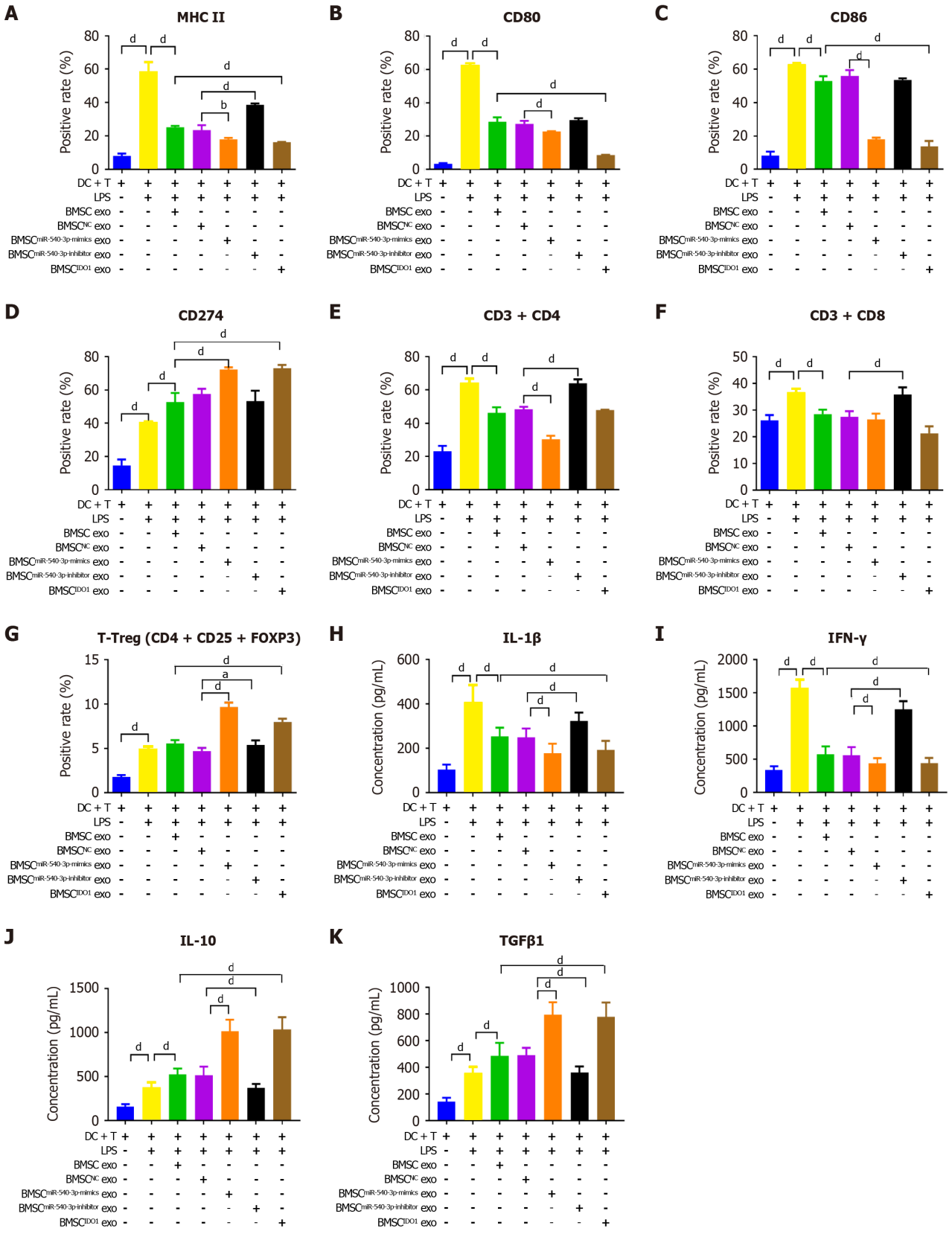

Figure 6 Effect of bone marrow mesenchymal stem cell$^{miR\text{-}540\text{-}3p\text{-}mimic}$ exosomes on dendritic cells after co-culturing with T cells. A-D: Flow cytometry analysis of the positive rate of cell surface markers (major histocompatibility complex II, CD80, CD86, and CD274) in dendritic cells cultured with T cells for 72 hours; E-G: Flow cytometry analysis of the positive rate of T cells ($CD4^+$ T, $CD8^+$ T, and T regulatory cells) and T cells after co-culture with dendritic cells; H-K: Enzyme-linked immunosorbent assay-based quantitative analysis of cytokine production (interleukin-1β, interferon-γ, interleukin-10, and transforming growth factor β 1) in dendritic cell-T cells co-cultures. $^aP < 0.05$, $^dP < 0.0001$. MHC: Major histocompatibility complex; BMSC: Bone marrow mesenchymal stem cell; IDO: Indoleamine 2,3-dioxygenase; DC: Dendritic cell; LPS: Lipopolysaccharide; exo: Exosomes; IL: Interleukin; TGF: Transforming growth factor; IFN: Interferon; Treg: T regulatory cell.

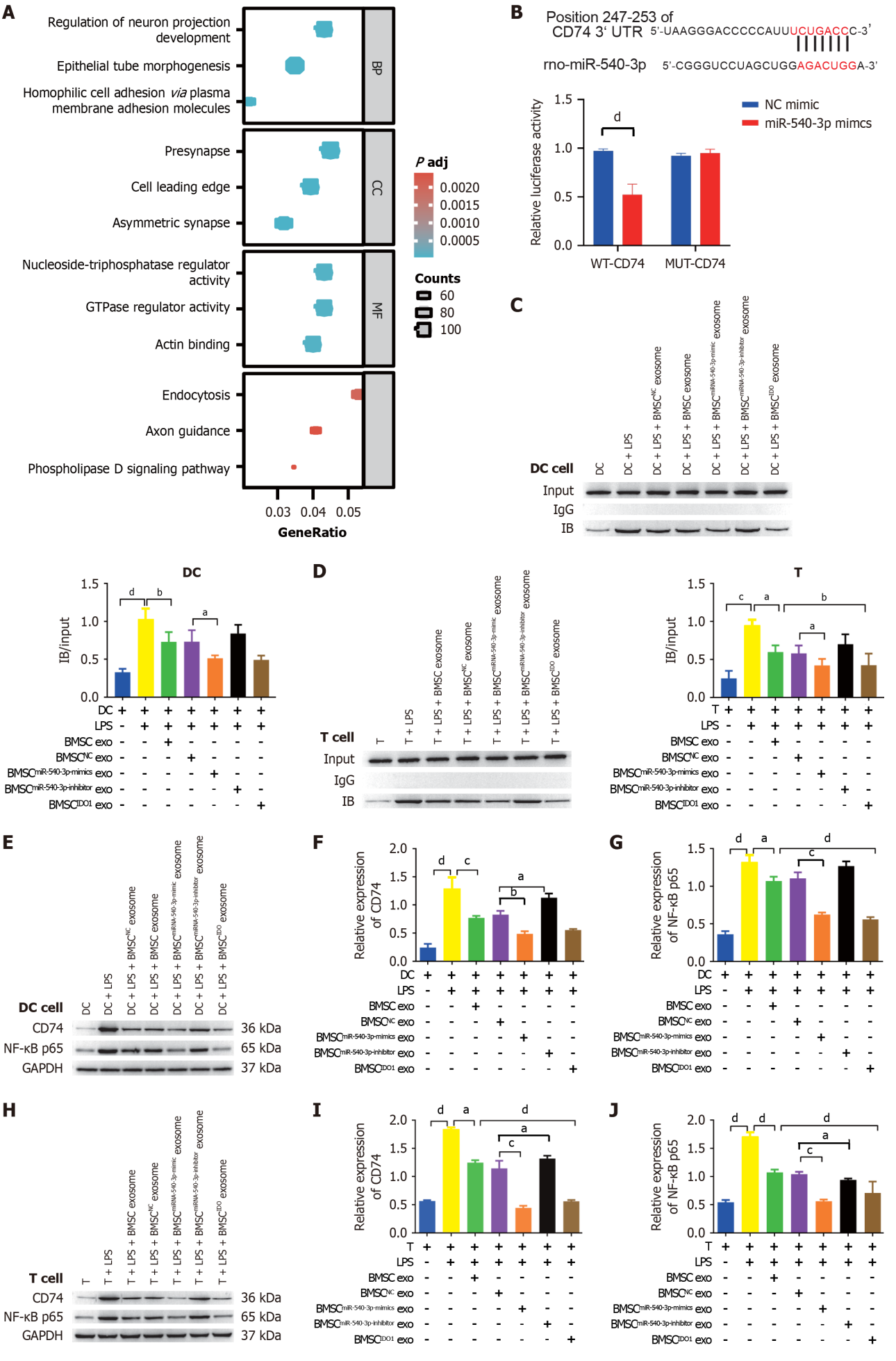
A
Regulation of neuron projection development
Epithelial tube morphogenesis
Homophilic cell adhesion *via* plasma membrane adhesion molecules
Presynapse
Cell leading edge
Asymmetric synapse
Nucleoside-triphosphatase regulator activity
GTPase regulator activity
Actin binding
Endocytosis
Axon guidance
Phospholipase D signaling pathway
BP
CC
MF
P adj
0.0020
0.0015
0.0010
0.0005
Counts
60
80
100
0.03 0.04 0.05
GeneRatio
B
Position 247-253 of CD74 3' UTR 5'-UAAGGGACCCCCAUUUCUGACCC-3'
rno-miR-540-3p 5'-CGGGUCCUAGCUGGAGACUGGA-3'
Relative luciferase activity
NC mimic
miR-540-3p mimcs
WT-CD74
MUT-CD74
C
DC cell
Input
IgG
IB
DC
DC + LPS
DC + LPS + BMSC^NC exosome
DC + LPS + BMSC exosome
DC + LPS + BMSC^miRNA-540-3p-mimic exosome
DC + LPS + BMSC^miRNA-540-3p-inhibitor exosome
DC + LPS + BMSC^IDO exosome
DC
IB/input
T cell
T
T + LPS
T + LPS + BMSC exosome
T + LPS + BMSC^NC exosome
T + LPS + BMSC^miRNA-540-3p-mimic exosome
T + LPS + BMSC^miRNA-540-3p-inhibitor exosome
T + LPS + BMSC^IDO exosome
T
BMSC exo
BMSC^NC exo
BMSC^miR-540-3p-mimics exo
BMSC^miR-540-3p-inhibitor exo
BMSC^IDO1 exo
E
DC cell
CD74
NF-κB p65
GAPDH
36 kDa
65 kDa
37 kDa
F
Relative expression of CD74
G
Relative expression of NF-κB p65
H
T cell
CD74
NF-κB p65
GAPDH
36 kDa
65 kDa
37 kDa
I
Relative expression of CD74
J
Relative expression of NF-κB p65

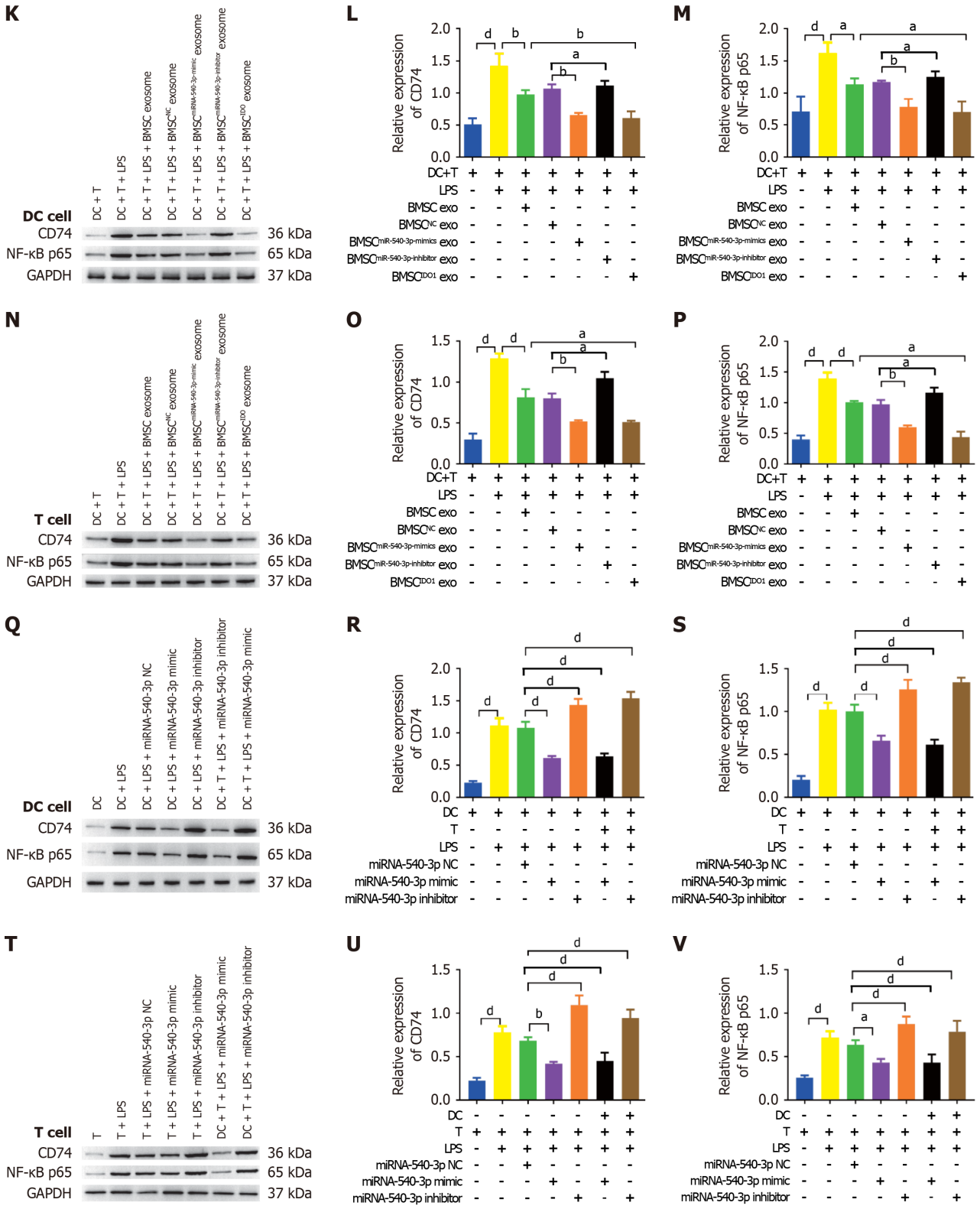

Figure 7 CD74 is a target of microRNA-540-3p and regulates P65 expression. A: Gene Ontology and Kyoto Encyclopedia of Genes and Genomes enrichment analyses of microRNA-540-3p (miR-540-3p) targets; B: A dual-luciferase assay was used to detect the binding of miR-540-3p to CD74; C: Co-IP was used to detect the binding of CD74 and nuclear factor-kappaB (NF-κB) in dendritic cells (DCs); D: Co-IP was used to detect the binding of CD74 and NF-κB in T cells; E-G: Western blot analysis of the expression of CD74 and NF-κB in DCs; H-J: Western blot analysis of the expression of CD74 and NF-κB in T cells; K-M: Western blot analysis of CD74 and NF-κB expression in DCs after co-culture with T cells; N-P: Western blot analysis of the expression of CD74 and NF-κB in T cells after co-culture with DCs; Q-S: Western blot analysis of the expression of CD74 and NF-κB in DCs after plasmid transfection; T-V: Western blot analysis of CD74 and NF-κB expression in T cells after plasmid transfection. $^{a}P < 0.05$, $^{b}P < 0.01$, $^{c}P < 0.001$, $^{d}P < 0.0001$. Mut: Mutant; BMSC: Bone marrow mesenchymal stem cell; IDO: Indoleamine 2,3-dioxygenase; DC: Dendritic cell; LPS: Lipopolysaccharide; exo: Exosomes; NF-κB: Nuclear factor-kappaB.

to examine how BMSC-derived exosomes with varying miR-540-3p levels influence immune tolerance.

Treatment of heart transplanted rats with BMSC$^{miR\text{-}540\text{-}3p\text{-}mimic}$ exosomes enhanced heart function

To determine the influence of miR-540-3p on immune resistance in an ectopic heart transplantation model, we respectively administered BMSC exosomes, BMSC$^{miR\text{-}540\text{-}3p\text{-}mimic}$ exosomes, BMSC$^{miR\text{-}540\text{-}3p\text{-}inhibitor}$ exosomes, BMSC^{NC} exosomes and BMSC^{IDO} exosomes *via* tail vein injection. Additionally, miR-540-3p knock-in and knock-out rats were generated, and an ectopic heart transplantation model was established in these rats. Histopathological examination of the grafted heart tissue was conducted in untransplanted WT SD rats (control) and SD rats undergoing Wistar-to-SD abdominal heterotopic heart transplantation.

In normal SD heart tissues, cardiomyocytes exhibit a neat arrangement with no inflammatory cells in the periphery of the blood vessels. Following ectopic heart transplantation, there was disorganization and reduction in cardiomyocytes, accompanied by severe infiltration of inflammatory cells in the transplantation model. In contrast to the BMSC exosome injection, the heart tissues from rats receiving BMSC$^{miR\text{-}540\text{-}3p\text{-}mimic}$ exosomes and BMSC^{IDO} exosomes exhibited a more ordered arrangement of cardiomyocytes, an increased number of cardiomyocytes, and milder infiltration of inflammatory cells. However, rats injected with BMSC$^{miR\text{-}540\text{-}3p\text{-}inhibitor}$ exosomes displayed a more disordered arrangement of cardiomyocytes, decreased cardiomyocyte numbers, and more severe infiltration of inflammatory cells. Compared to the models established using normal SD rats and miR-540-3p knock-in rats, the latter exhibited a milder pathology with a more ordered arrangement, increased cardiomyocyte numbers, and less infiltration of inflammatory cells. Conversely, the model established using miR-540-3p knock-out rats displayed more severe pathology, including a more disordered arrangement, decreased cardiomyocyte numbers, and more pronounced infiltration of inflammatory cells (Figure 8A).

Echocardiography revealed that following BMSC exosome injection, the ejection fraction and ratio of fraction shortening significantly increased compared to those in the model group. Injection of BMSC$^{miR\text{-}540\text{-}3p\text{-}mimic}$ exosomes and BMSC^{IDO} exosomes further increased the ejection fraction and ratio of fraction shortening. Compared to the WT model, miR-540-3p knock-in rats exhibited an increased ejection fraction and ratio of fraction shortening, whereas miR-540-3p knock-out rats showed a decrease in both parameters (Figure 8B and C). Following the observed improvements in cardiac function, we next examined changes in serum cytokine levels to better understand the systemic immune response induced by BMSC-derived exosomes. Compared to normal SD rats, the ectopic heart transplantation model exhibited increased serum levels of IL-1β, IFN-γ, IL-10, and TGFβ1. Following the injection of BMSC exosomes, there was a decrease in the serum concentrations of IL-1β and IFN-γ. When administered BMSC$^{miR\text{-}540\text{-}3p\text{-}mimic}$ exosomes, the serum concentrations of IL-1β and IFN-γ decreased, whereas those of IL-10 and TGFβ1 increased. In contrast, injection of BMSC$^{miR\text{-}540\text{-}3p\text{-}inhibitor}$ exosomes led to an increase in serum concentrations of IL-1β and IFN-γ, accompanied by a decrease in TGFβ1 compared with the BMSC exosome injection group. Injection of BMSC^{IDO} exosomes resulted in an increase in serum concentrations of IL-10 and TGFβ1 (Figure 8D-G). These findings suggest that specific miR-540-3p-modulated exosomes can influence systemic cytokine profiles, supporting an immune-tolerant environment.

Subsequently, DCs and T cells were extracted from the spleen, and qPCR was performed to detect the expression of miR-540-3p. Relative to normal WT SD rats, the heterotopic heart transplantation model exhibited decreased expression of miR-540-3p in extracted DCs and T cells. Administration of BMSC exosomes increased the expression of miR-540-3p in extracted DCs and T cells. Further elevation in the expression of miR-540-3p in the extracted DCs and T cells occurred when BMSC$^{miR\text{-}540\text{-}3p\text{-}mimic}$ exosomes and BMSC^{IDO} exosomes were administered. Conversely, injection of BMSC$^{miR\text{-}540\text{-}3p\text{-}inhibitor}$ exosomes resulted in a decrease in the expression of miR-540-3p in extracted DCs and T cells compared to the BMSC exosome injection group. Compared to the WT model, miR-540-3p knock-in rats exhibited increased expression of miR-540-3p in DCs and T cells, whereas miR-540-3p knock-out rats displayed decreased expression of miR-540-3p (Figure 8H and I). These findings indicate that miR-540-3p expression levels are modulated by BMSC exosome treatment and may play a crucial role in regulating immune responses in the transplantation model.

To further elucidate the molecular mechanisms underlying these immune responses, we investigated changes in T cell subpopulations as well as the expression of key immune regulatory proteins CD74 and NF-κB p65. In the WT model group, there was an increase in the positive rate of CD80, CD86, MHC II, and CD274, as well as in the ratio of $CD4^+$ T cells, $CD8^+$ T cells, and Tregs, compared to normal SD rats. Following BMSC exosome injection, the positive rates of CD80, CD86, and MHC II, along with the ratio of $CD4^+$ T cells to $CD8^+$ T cells, decreased, while the positive rate of CD274 and the ratio of Tregs increased compared to those in the WT model. Further decreases in the positive rate of CD80, CD86, and MHC II, as well as the ratio of $CD4^+$ T cells to $CD8^+$ T cells, were observed following the injection of BMSC$^{miR\text{-}540\text{-}3p\text{-}mimic}$ exosomes and BMSC^{IDO} exosomes. Conversely, the positivity rate of CD274 and the ratio of Tregs increased further compared to those in the BMSC exosome injection group. The injection of BMSC$^{miR\text{-}540\text{-}3p\text{-}inhibitor}$ exosomes increased the positivity rates of CD80 and CD86, along with the ratio of $CD4^+$ and $CD8^+$ T cells. Conversely, the positivity rate of CD274 and the ratio of Tregs decreased compared to those in the BMSC exosome-injected group. Compared to the WT model, the positive rates of CD80, CD86, and MHC II, along with the ratio of $CD4^+$ T cells to $CD8^+$ T cells, decreased in the extracted DCs and T cells. Conversely, the positivity rate of CD274 and the ratio of Tregs increased in miR-540-3p knock-in rats, whereas the positivity rate of CD274 and the ratio of Tregs decreased in miR-540-3p knock-out rats (Figure 8J-P, Supplementary Figure 4). Western blotting was performed to assess the expression of CD74 and NF-κB p65. Relative to WT normal SD rats, the heterotopic heart transplantation model exhibited an increase in the expression of CD74 and NF-κB p65 in DCs and T cells. Following the injection of BMSC exosomes, there was a decrease in the expression of CD74 and NF-κB p65 in the extracted DCs and T cells. Administration of BMSC$^{miR\text{-}540\text{-}3p\text{-}mimic}$ exosomes and BMSC^{IDO} exosomes resulted in a further decrease in the expression of CD74 and NF-κB p65 in extracted DCs and T cells. Conversely, injection of BMSC$^{miR\text{-}540\text{-}3p\text{-}inhibitor}$ exosomes led to an increase in the expression of CD74 and NF-κB p65 in extracted DCs and T cells compared to the BMSC exosome injection group (Figure 8Q-V).

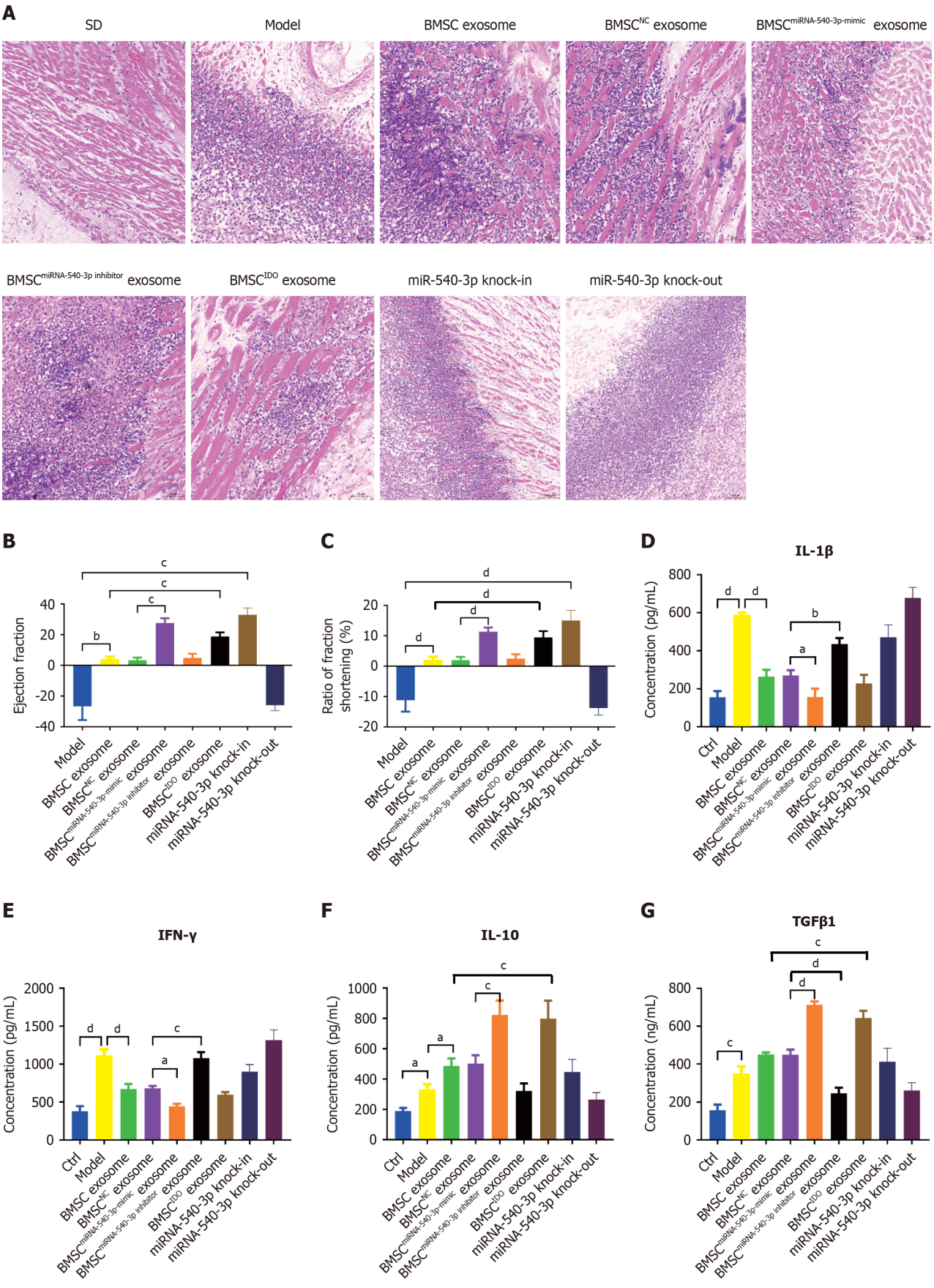
A
SD
Model
BMSC exosome
BMSC^{NC} exosome
BMSC$^{miRNA-540-3p-mimic}$ exosome
BMSC$^{miRNA-540-3p\ inhibitor}$ exosome
BMSC^{IDO} exosome
miR-540-3p knock-in
miR-540-3p knock-out
B
Ejection fraction
C
Ratio of fraction shortening (%)
D
IL-1β
Concentration (pg/mL)
E
IFN-γ
Concentration (pg/mL)
F
IL-10
Concentration (pg/mL)
G
TGFβ1
Concentration (ng/mL)
Ctrl
Model
BMSC exosome
BMSC^{NC} exosome
BMSC$^{miRNA-540-3p-mimic}$ exosome
BMSC$^{miRNA-540-3p\ inhibitor}$ exosome
BMSC^{IDO} exosome
miRNA-540-3p knock-in
miRNA-540-3p knock-out

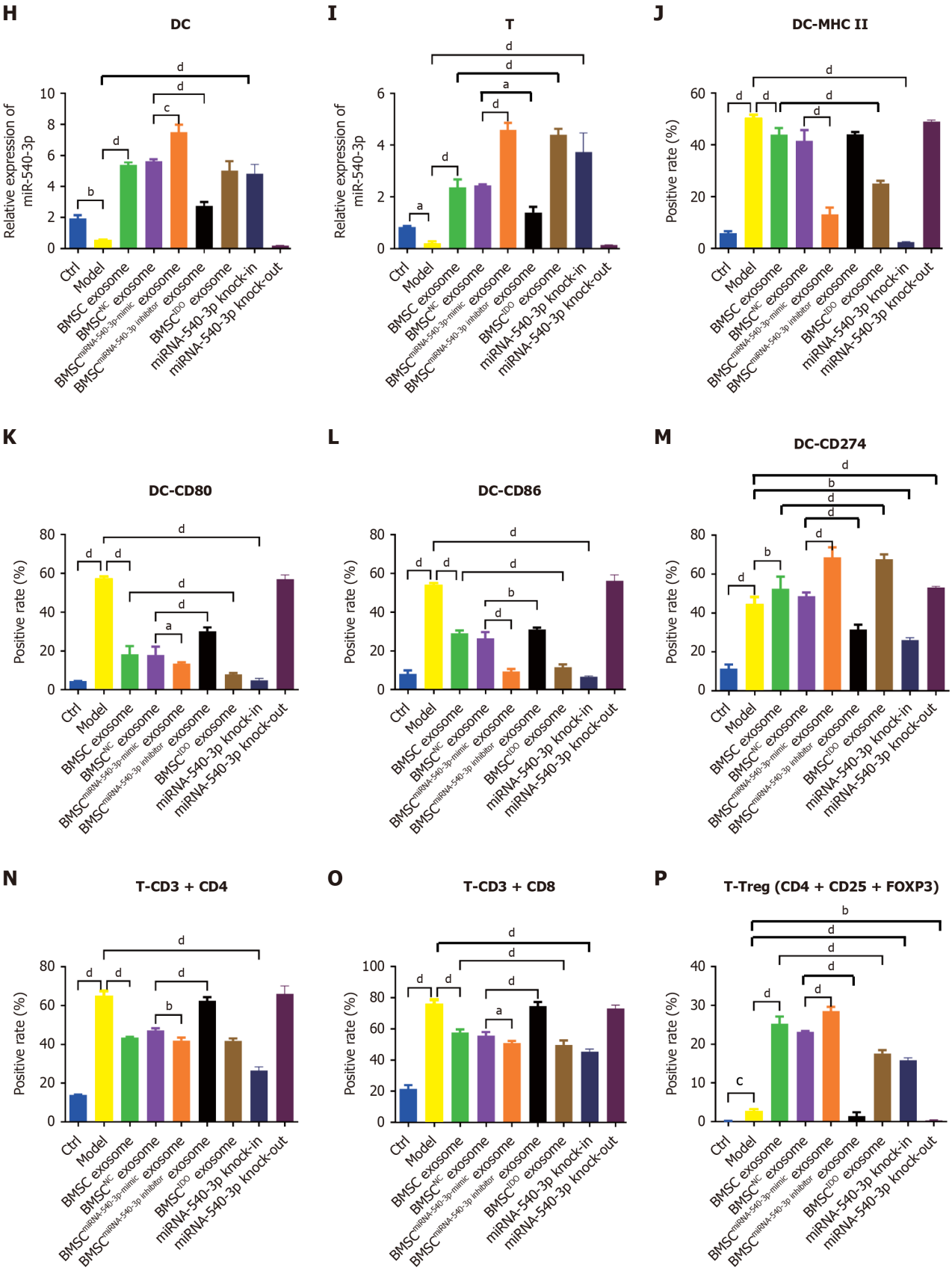
H
DC
Relative expression of miR-540-3p
I
T
Relative expression of miR-540-3p
J
DC-MHC II
Positive rate (%)
K
DC-CD80
Positive rate (%)
L
DC-CD86
Positive rate (%)
M
DC-CD274
Positive rate (%)
N
T-CD3 + CD4
Positive rate (%)
O
T-CD3 + CD8
Positive rate (%)
P
T-Treg (CD4 + CD25 + FOXP3)
Positive rate (%)
Ctrl
Model
BMSC exosome
BMSC^NC exosome
BMSC^miRNA-540-3p-mimic exosome
BMSC^miRNA-540-3p inhibitor exosome
BMSC^IDO exosome
miRNA-540-3p knock-in
miRNA-540-3p knock-out

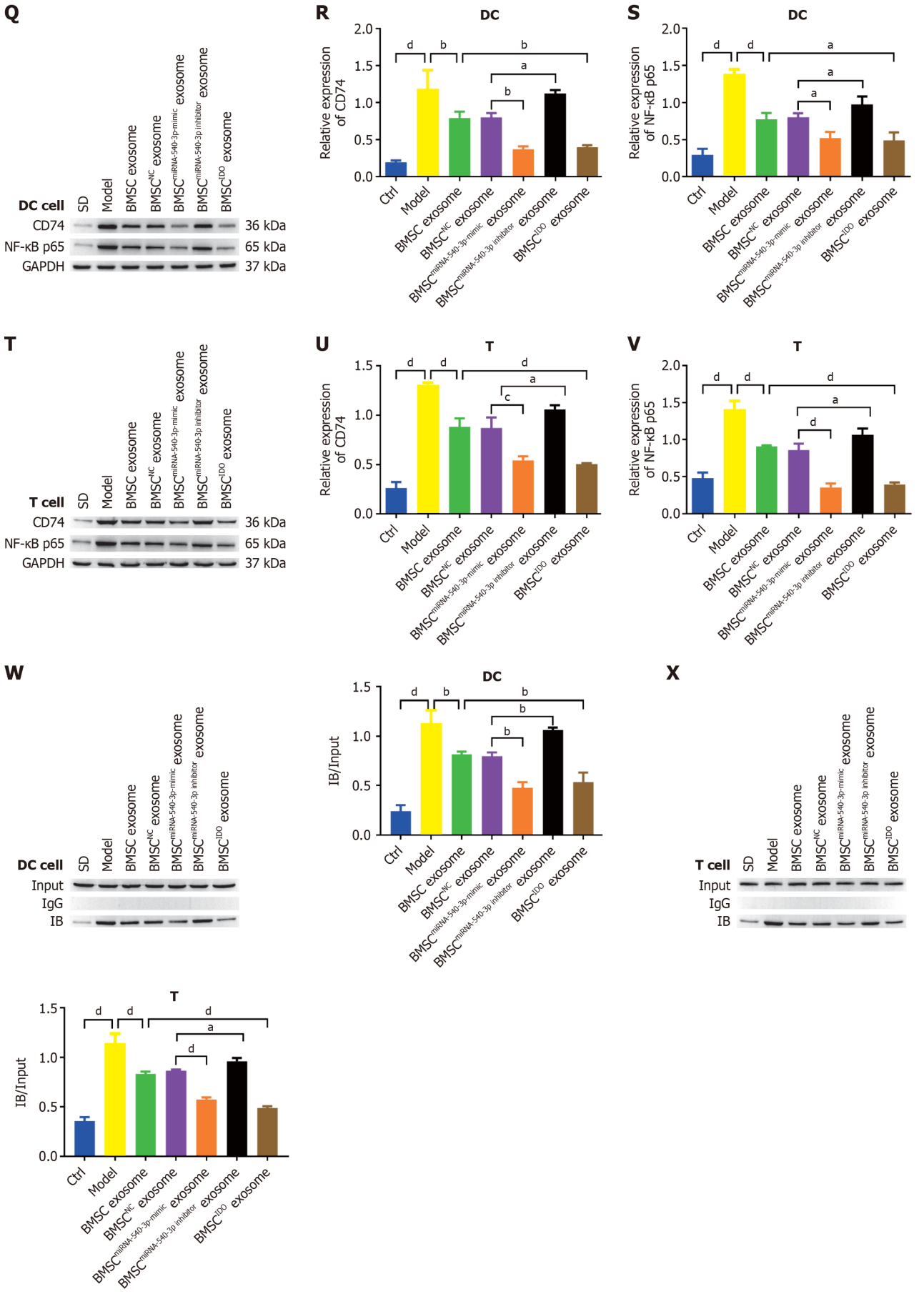

Figure 8 Exosome-derived miR-540-3p alleviates immune resistance after heterotopic heart transplantation. A: Histopathological observation of the heart after heterotopic heart transplantation using hematoxylin and eosin staining; B: Detection and calculation of the difference in ejection fraction before and

after heterotopic heart transplantation; C: Detection and calculation of differences in the percentage of fractional shortening before and after heterotopic heart transplantation; D-G: Enzyme-linked immunosorbent assay-based quantitative analysis of cytokine production (interleukin-1β, interferon-γ, interleukin-10, transforming growth factor β1) in serum; H: Expression of microRNA-540-3p in extracted dendritic cells (DCs); I: Expression of microRNA-540-3p in extracted T cells; J-M: Flow cytometric analysis of the positive rate of cell surface markers in DCs (major histocompatibility complex II, CD80, CD86, and CD274); N-P: Flow cytometric analysis of the positive rate of T cells ($CD4^+$ T, $CD8^+$ T, and T regulatory cells); Q-S: Western blot analysis of the expression of CD74 and nuclear factor-kappaB (NF-κB) in extracted DCs; T-V: Western blot analysis of CD74 and NF-κB expression in the extracted T cells; W: Co-IP was used to detect the binding of CD74 and NF-κB in extracted DCs; X: Co-IP was used to detect the binding of CD74 and NF-κB in extracted T cells. $^aP < 0.05$, $^bP < 0.01$, $^cP < 0.001$, $^dP < 0.0001$. BMSC: Bone marrow mesenchymal stem cell; IDO: Indoleamine 2,3-dioxygenase; DC: Dendritic cell; LPS: Lipopolysaccharide; NF-κB: Nuclear factor-kappaB; MHC: Major histocompatibility complex; IL: Interleukin; TGF: Transforming growth factor; IFN: Interferon.

The interaction between CD74 and NF-κB p65 was verified through a co-immunoprecipitation experiment following transfection of CD74 and NF-κB p65 in DCs and T cells. These results demonstrated the co-precipitation of CD74 with NF-κB p65. In the established model, the precipitate was more pronounced and decreased upon injection of BMSC exosomes. This reduction was further observed with $BMSC^{miR\text{-}540\text{-}3p\text{-}mimic}$ and $BMSC^{IDO}$ exosome injections, while an increase was noted with $BMSC^{miR\text{-}540\text{-}3p\text{-}inhibitor}$ exosome injection, compared to the BMSC exosome injection group (Figure 8W and X). These findings indicate that treatment of heart-transplanted rats with $BMSC^{miR\text{-}540\text{-}3p\text{-}mimic}$ exosomes enhanced immune tolerance. Moreover, miR-540-3p was identified as a negative regulator of the CD74-NF-κB axis, leading to the altered phenotype of DCs and T cells (Figure 9). In summary, these findings indicate that treatment of heart-transplanted rats with $BMSC^{miR\text{-}540\text{-}3p\text{-}mimic}$ exosomes enhanced immune tolerance, largely by modulating the CD74-NF-κB axis, which in turn altered the phenotypes of DCs and T cells to support an immune-tolerant environment.

DISCUSSION

This study investigated the immunosuppressive properties of exosomes derived from miR-540-3p-overexpressing BMSCs in the context of allograft transplantation. Our findings revealed that miR-540-3p, by inhibiting the CD74/NF-κB axis, significantly altered the phenotype of DCs and T cells, promoting a shift towards an anti-inflammatory cytokine profile and enhancing immune tolerance in the transplanted heart.

Inflammation plays a central role in the pathogenesis of numerous acute and chronic diseases. NF-κB, a key transcription factor in the inflammatory response, drives the expression of several pro-inflammatory genes, including cytokines such as IL-1β, TNF-α, IFN-γ, and IL-10, which are critical in disease progression. Our results demonstrate that miR-540-3p, *via* exosomes, effectively downregulated the expression of CD74 and NF-κB, leading to a suppressed pro-inflammatory response. This finding not only has implications for organ transplantation but also suggests potential therapeutic applications of miR-540-3p in other inflammation-related diseases. CD74, a type II transmembrane glycoprotein, plays a crucial role in the MHC II antigen presentation pathway and immune cell activation[43,44]. Studies indicate that CD74 induces B cell maturation through the NF-κB p65/RelA homodimer and its coactivator TAFII[51,52]. Furthermore, CD74 serves as the primary receptor for the pro-inflammatory cytokine macrophage migration inhibitory factor. Binding of migration inhibitory factor to the CD74/CD44 receptor complex activates extracellular signal-regulated kinase 1/2 in the mitogen-activated protein kinases pathway and phosphoinositide 3-kinase/Akt/SRC signal transduction cascade, influencing the activity of macrophages, DCs, T cells, and B cells[43,44]. NF-κB, a downstream signaling molecule of CD74, is known to be activated in macrophages when exposed to inflammatory stimuli such as LPS, influencing gene expression involved in macrophage-mediated immune responses, including inflammation, cell differentiation, migration, and survival[53]. In atherosclerosis, NF-κB inhibition may reduce inflammatory cell infiltration in the arterial walls, slowing plaque development[53]. Similarly, in cancer, the miR-540-3p-mediated regulation of the CD74/NF-κB axis could reduce immune evasion by tumor cells, potentially enhancing the effectiveness of immunotherapies[43,44].

Exosomes, as key mediators of intercellular communication, play crucial roles in inflammation by delivering miRNAs, proteins, and other bioactive molecules that modulate the functional state of recipient cells. Exosomes from miR-540-3p-overexpressing BMSCs not only suppressed pro-inflammatory activity of DCs and T cells *in vitro* but also reduced inflammatory cell infiltration *in vivo* in the transplanted heart, demonstrating their potent anti-inflammatory and immune regulatory capacity. It is widely acknowledged that MSC-derived exosomes have immunomodulatory property, involved in the immune cell proliferation, differentiation, or activation. For instance, Blazquez *et al*[54] reported that adipose MSC-derived exosomes inhibit T cell differentiation and activation, reduce T cell proliferation, and suppress IFN-γ secretion. Chen *et al*[33] demonstrated that healthy BMSCs derived exosomes could inhibit the secretion of the pro-inflammatory cytokines TNF-α and IL-1β, elevate the level of the anti-inflammatory cytokine TGFβ, induce the conversion of type 1 helper T (Th1) into Th2, diminish the differentiation of naïve T cells into Th17 cells, and augment the number of Tregs. Similarly, Ma *et al*[55] demonstrated that exosomes obtained from MSCs cultured in a defined medium decreased the concentration of pro-inflammatory cytokines IFN-γ and IL-1β, while increasing anti-inflammatory cytokines TGFβ1 and IL-10. Hu *et al*[56] observed that exosomes from cord blood-derived stem cells downregulated $CD4^+$ T and $CD8^+$ T cells, upregulated Tregs, reduced the co-stimulating molecules CD80 and CD86, and increased the immune tolerance-related marker CD274. Moreover, Xu *et al*[30] showed that exosomes derived from LPS-preconditioned BMSCs decreased M1 macrophage polarization, increased M2 macrophage polarization, suppressed the LPS-dependent NF-κB signaling pathway, and partially activated the AKT1/AKT2 signaling pathway, especially under LPS stimulation.

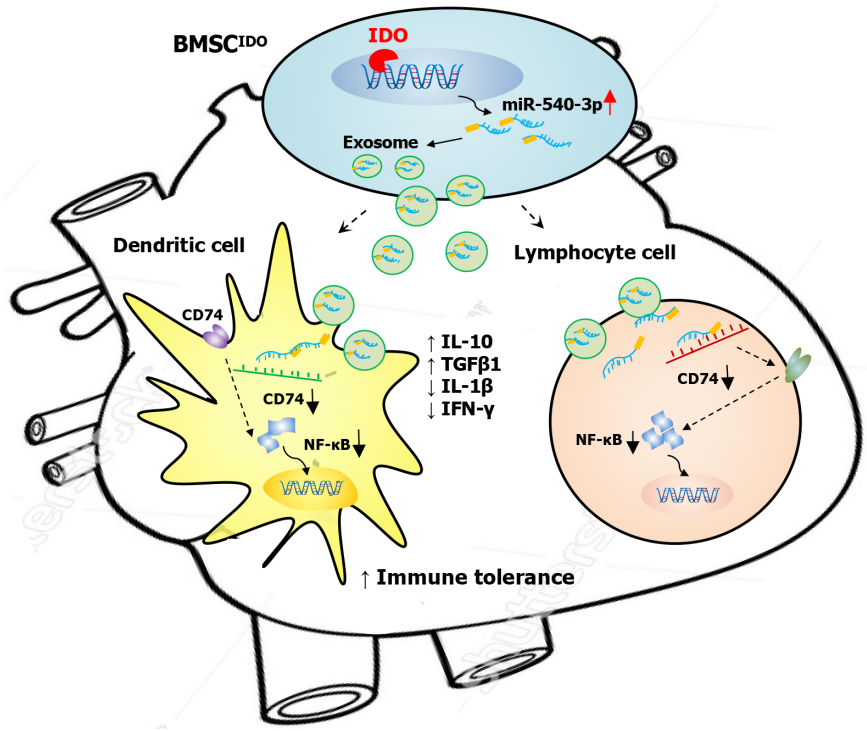

Figure 9 Exosomes derived from microRNA-540-3p overexpressing bone marrow mesenchymal stem cells promote immune tolerance to cardiac allograft *via* the CD74/nuclear factor-kappaB pathway. BMSC: Bone marrow mesenchymal stem cell; IDO: Indoleamine 2,3-dioxygenase; IL: Interleukin; TGF: Transforming growth factor; IFN: Interferon; NF-κB: Nuclear factor-kappaB.

To validate these *in vitro* findings, we extended our investigation to an *in vivo* rat heterotopic heart transplantation model. Rats undergoing heterotopic heart transplantation were treated with exosomes derived from different BMSCs, including miR-540-3p-knock-in and miR-540-3p-knock-out transplanted rats. Our *in vivo* findings are consistent with previous studies showing that MSC-derived exosomes reduce inflammation and improve heart function in a rat MI model, with this effect being superior to that using MSCs alone[55]. Our results also align with findings from Xu *et al*[30], demonstrating that exosomes from LPS-preconditioned BMSCs attenuate post-infarction inflammation and reduce myocardial injury in a mouse model of MI.

Our previous study demonstrated that exosomes derived from IDO-overexpressing BMSCs promoted immune tolerance in a rat heterotopic heart transplantation model[41]. In that study, we identified miR-540-3p as the most upregulated miRNA in exosomes derived from IDO-overexpressing BMSCs compared with exosomes from other groups. The present study further indicates that exosomes from miR-540-3p-overexpressing BMSCs exhibit immunomodulatory effects comparable to those of exosomes from IDO-overexpressing BMSCs, supporting the importance of miR-540-3p in this immune regulatory pathway. IDO is a potent immunomodulator activated in APCs (*e.g.*, DCs, macrophages, and B cells), leading to the suppression of T effector cells and induction of Tregs[57]. Given the elevated expression of miR-540-3p in exosomes derived from IDO-overexpressing BMSCs and the similar immunomodulatory effects exerted by miR-540-3p alone, we suggest that miR-540-3p participates in IDO-mediated immunosuppression and cardiac allograft tolerance, possibly through a CD74/NF-κB-dependent mechanism.

Our findings showed that cytokines including IL-1β, IFN-γ, TGFβ1, and IL-10 were modulated by miR-540-3p. Considering our results, the upregulation of IFN-γ is related to the increased ratio of $CD4^+$ and $CD8^+$ T cells[58,59], and the downregulation of TGFβ1 is related with the reduced ratio of Tregs[59,60]. The mechanism underlying the modulation of IL-1β1 and IL-10 by miR-540-3p remains further investigation, possibly related with a cross-talk between signal transducer and activator of transcription and NF-κB pathway[61].

CONCLUSION

Our findings revealed that miR-540-3p can modulate the activity of DCs and T cells, diminish the expression of CD74 and NF-κB, and suppress inflammatory responses by reducing pro-inflammatory cytokines while increasing anti-inflammatory cytokines, both *in vitro* and *in vivo*. Furthermore, miR-540-3p has been shown to enhance heart function and protect grafted hearts in a rat model. This study highlights the therapeutic potential of exosomes derived from miR-540-3p-overexpressing BMSCs and presents a cell-free strategy to foster immune tolerance in cardiac allografts.

ACKNOWLEDGEMENTS

We borrowed the animal experiment platform due to the limitations of the platform in our affiliations. Our co-author, Ji-Gang He performed animal experiments with the supervision of ethnic Committee of the Yunan Labreal Biotech Ltd, co. Specially thanks for their help.

FOOTNOTES

Author contributions: He JG and Mao FG contributed to the conceptualization of this manuscript; He JG and Wu XX participated in the software; He JG and Xiao GP were involved in the investigation of this study; He JG and Li S wrote the original draft; Li S contributed to the data curation; He JG participated in the methodology, funding acquisition, formal analysis of this manuscript; Li S and Yan D contributed to the visualization; Xiao GP and Mao FG were involved in the resources and supervision; Wu XX contributed to the validation; Yan D and Mao FG contributed to the writing - review & editing; Mao FG took part in resources and supervision.

Supported by the National Natural Science Foundation of China, No. 82060299; Medical Discipline Leader Project of Yunnan Provincial Health Commission, No. D-2019020; Yunnan Provincial Government Ten Thousand Person-Top Young Talents Project, No. KH-SWR-QNBJ-2019-002; Clinical Medical Center of the First People's Hospital of Yunnan Province, No. 2021LCZXXF-XZ04 and No. 2022LCZXKF-HX05; Kunming Medical Joint Special Project - Outstanding Youth Cultivation Project, No. 202101AY070001-034; Kunming Medical Joint Special Project, No. 202101AY070001-272; Famous Doctor Project of "Xingdian Talent Support Plan" of Yunnan Province, No. XDYC-MY-2022-0037; and Yunnan Province 2023 Undergraduate Education and Teaching Reform Research Project, No. 2023BKXJJG-F04002.

Institutional animal care and use committee statement: All animal experiments were performed with the help of Yunan Labreal Biotech Ltd, co. in accordance with the ARRIVE principles and were approved by the Animal Care and Use Committee of the Yunan Labreal Biotech Ltd, co. Approval number: No. SL20220510.

Conflict-of-interest statement: The Yunan Labreal Biotech Ltd, co. provided the research materials in the animal experiment. Although the animal experiment was performed in the platform of a private company, they did not aware of or interfere the experimental propose and not participate in the writing, review, and publication of this manuscript. No economic interests were appeared.

Data sharing statement: The datasets used and/or analyzed during the current study are available from the corresponding author upon reasonable request.

ARRIVE guidelines statement: The authors have read the ARRIVE guidelines, and the manuscript was prepared and revised according to the ARRIVE guidelines.

Country of origin: China

ORCID number: Fu-Gang Mao 0009-0007-7625-839X.

S-Editor: Wang JJ
L-Editor: A
P-Editor: Zheng XM

REFERENCES

1 **Savarese G**, Lund LH. Global Public Health Burden of Heart Failure. *Card Fail Rev* 2017; **3**: 7-11 [PMID: 28785469 DOI: 10.15420/cfr.2016:25:2]
2 **Katz JN**, Waters SB, Hollis IB, Chang PP. Advanced therapies for end-stage heart failure. *Curr Cardiol Rev* 2015; **11**: 63-72 [PMID: 24251460 DOI: 10.2174/1573403x09666131117163825]
3 **Mcdermott JK**. Complications of Immunosuppression. In: Bogar L, Stempien-Otero A. Contemporary Heart Transplantation. Organ and Tissue Transplantation. Cham: Springer, 2020
4 **Hasegawa H**, Matsumoto T. Mechanisms of Tolerance Induction by Dendritic Cells In Vivo. *Front Immunol* 2018; **9**: 350 [PMID: 29535726 DOI: 10.3389/fimmu.2018.00350]
5 **Zhang X**, Li M, Lian D, Zheng X, Zhang ZX, Ichim TE, Xia X, Huang X, Vladau C, Suzuki M, Garcia B, Jevnikar AM, Min WP. Generation of therapeutic dendritic cells and regulatory T cells for preventing allogeneic cardiac graft rejection. *Clin Immunol* 2008; **127**: 313-321 [PMID: 18358783 DOI: 10.1016/j.clim.2008.01.013]
6 **Kopecky BJ**, Dun H, Amrute JM, Lin CY, Bredemeyer AL, Terada Y, Bayguinov PO, Koenig AL, Frye CC, Fitzpatrick JAJ, Kreisel D, Lavine KJ. Donor Macrophages Modulate Rejection After Heart Transplantation. *Circulation* 2022; **146**: 623-638 [PMID: 35880523 DOI:

10.1161/CIRCULATIONAHA.121.057400]

7 **Song X**, Xie S, Lu K, Wang C. Mesenchymal stem cells alleviate experimental asthma by inducing polarization of alveolar macrophages. *Inflammation* 2015; **38**: 485-492 [PMID: 24958014 DOI: 10.1007/s10753-014-9954-6]

8 **Spaggiari GM**, Abdelrazik H, Becchetti F, Moretta L. MSCs inhibit monocyte-derived DC maturation and function by selectively interfering with the generation of immature DCs: central role of MSC-derived prostaglandin E2. *Blood* 2009; **113**: 6576-6583 [PMID: 19398717 DOI: 10.1182/blood-2009-02-203943]

9 **Khan I**, Zhang L, Mohammed M, Archer FE, Abukharmah J, Yuan Z, Rizvi SS, Melek MG, Rabson AB, Shi Y, Weinberger B, Vetrano AM. Effects of Wharton's jelly-derived mesenchymal stem cells on neonatal neutrophils. *J Inflamm Res* 2015; **8**: 1-8 [PMID: 25678809 DOI: 10.2147/JIR.S71987]

10 **Qu M**, Cui J, Zhu J, Ma Y, Yuan X, Shi J, Guo D, Li C. Bone marrow-derived mesenchymal stem cells suppress NK cell recruitment and activation in PolyI:C-induced liver injury. *Biochem Biophys Res Commun* 2015; **466**: 173-179 [PMID: 26342798 DOI: 10.1016/j.bbrc.2015.08.125]

11 **Coulson-Thomas VJ**, Gesteira TF, Hascall V, Kao W. Umbilical cord mesenchymal stem cells suppress host rejection: the role of the glycocalyx. *J Biol Chem* 2014; **289**: 23465-23481 [PMID: 24986866 DOI: 10.1074/jbc.M114.557447]

12 **Fu QL**, Chow YY, Sun SJ, Zeng QX, Li HB, Shi JB, Sun YQ, Wen W, Tse HF, Lian Q, Xu G. Mesenchymal stem cells derived from human induced pluripotent stem cells modulate T-cell phenotypes in allergic rhinitis. *Allergy* 2012; **67**: 1215-1222 [PMID: 22882409 DOI: 10.1111/j.1398-9995.2012.02875.x.]

13 **Rosado MM**, Bernardo ME, Scarsella M, Conforti A, Giorda E, Biagini S, Cascioli S, Rossi F, Guzzo I, Vivarelli M, Dello Strologo L, Emma F, Locatelli F, Carsetti R. Inhibition of B-cell proliferation and antibody production by mesenchymal stromal cells is mediated by T cells. *Stem Cells Dev* 2015; **24**: 93-103 [PMID: 25036865 DOI: 10.1089/scd.2014.0155]

14 **Caplan AI**, Dennis JE. Mesenchymal stem cells as trophic mediators. *J Cell Biochem* 2006; **98**: 1076-1084 [PMID: 16619257 DOI: 10.1002/jcb.20886]

15 **Kinnaird T**, Stabile E, Burnett MS, Shou M, Lee CW, Barr S, Fuchs S, Epstein SE. Local delivery of marrow-derived stromal cells augments collateral perfusion through paracrine mechanisms. *Circulation* 2004; **109**: 1543-1549 [PMID: 15023891 DOI: 10.1161/01.CIR.0000124062.31102.57]

16 **Giebel B**, Kordelas L, Börger V. Clinical potential of mesenchymal stem/stromal cell-derived extracellular vesicles. *Stem Cell Investig* 2017; **4**: 84 [PMID: 29167805 DOI: 10.21037/sci.2017.09.06]

17 **Zheng Q**, Zhang S, Guo WZ, Li XK. The Unique Immunomodulatory Properties of MSC-Derived Exosomes in Organ Transplantation. *Front Immunol* 2021; **12**: 659621 [PMID: 33889158 DOI: 10.3389/fimmu.2021.659621]

18 **Eggenhofer E**, Benseler V, Kroemer A, Popp FC, Geissler EK, Schlitt HJ, Baan CC, Dahlke MH, Hoogduijn MJ. Mesenchymal stem cells are short-lived and do not migrate beyond the lungs after intravenous infusion. *Front Immunol* 2012; **3**: 297 [PMID: 23056000 DOI: 10.3389/fimmu.2012.00297]

19 **Zitvogel L**, Regnault A, Lozier A, Wolfers J, Flament C, Tenza D, Ricciardi-Castagnoli P, Raposo G, Amigorena S. Eradication of established murine tumors using a novel cell-free vaccine: dendritic cell-derived exosomes. *Nat Med* 1998; **4**: 594-600 [PMID: 9585234 DOI: 10.1038/nm0598-594]

20 **Raposo G**, Nijman HW, Stoorvogel W, Liejendekker R, Harding CV, Melief CJ, Geuze HJ. B lymphocytes secrete antigen-presenting vesicles. *J Exp Med* 1996; **183**: 1161-1172 [PMID: 8642258 DOI: 10.1084/jem.183.3.1161]

21 **Peters PJ**, Geuze HJ, Van der Donk HA, Slot JW, Griffith JM, Stam NJ, Clevers HC, Borst J. Molecules relevant for T cell-target cell interaction are present in cytolytic granules of human T lymphocytes. *Eur J Immunol* 1989; **19**: 1469-1475 [PMID: 2789142 DOI: 10.1002/eji.1830190819]

22 **Lai RC**, Arslan F, Lee MM, Sze NS, Choo A, Chen TS, Salto-Tellez M, Timmers L, Lee CN, El Oakley RM, Pasterkamp G, de Kleijn DP, Lim SK. Exosome secreted by MSC reduces myocardial ischemia/reperfusion injury. *Stem Cell Res* 2010; **4**: 214-222 [PMID: 20138817 DOI: 10.1016/j.scr.2009.12.003]

23 **Lener T**, Gimona M, Aigner L, Börger V, Buzas E, Camussi G, Chaput N, Chatterjee D, Court FA, Del Portillo HA, O'Driscoll L, Fais S, Falcon-Perez JM, Felderhoff-Mueser U, Fraile L, Gho YS, Görgens A, Gupta RC, Hendrix A, Hermann DM, Hill AF, Hochberg F, Horn PA, de Kleijn D, Kordelas L, Kramer BW, Krämer-Albers EM, Laner-Plamberger S, Laitinen S, Leonardi T, Lorenowicz MJ, Lim SK, Lötvall J, Maguire CA, Marcilla A, Nazarenko I, Ochiya T, Patel T, Pedersen S, Pocsfalvi G, Pluchino S, Quesenberry P, Reischl IG, Rivera FJ, Sanzenbacher R, Schallmoser K, Slaper-Cortenbach I, Strunk D, Tonn T, Vader P, van Balkom BW, Wauben M, Andaloussi SE, Théry C, Rohde E, Giebel B. Applying extracellular vesicles based therapeutics in clinical trials - an ISEV position paper. *J Extracell Vesicles* 2015; **4**: 30087 [PMID: 26725829 DOI: 10.3402/jev.v4.30087]

24 **Ahmed L**, Al-Massri K. New Approaches for Enhancement of the Efficacy of Mesenchymal Stem Cell-Derived Exosomes in Cardiovascular Diseases. *Tissue Eng Regen Med* 2022; **19**: 1129-1146 [PMID: 35867309 DOI: 10.1007/s13770-022-00469-x]

25 **Suzuki E**, Fujita D, Takahashi M, Oba S, Nishimatsu H. Stem cell-derived exosomes as a therapeutic tool for cardiovascular disease. *World J Stem Cells* 2016; **8**: 297-305 [PMID: 27679686 DOI: 10.4252/wjsc.v8.i9.297]

26 **Cheng L**, Zhang K, Wu S, Cui M, Xu T. Focus on Mesenchymal Stem Cell-Derived Exosomes: Opportunities and Challenges in Cell-Free Therapy. *Stem Cells Int* 2017; **2017**: 6305295 [PMID: 29410682 DOI: 10.1155/2017/6305295]

27 **Ju C**, Shen Y, Ma G, Liu Y, Cai J, Kim IM, Weintraub NL, Liu N, Tang Y. Transplantation of Cardiac Mesenchymal Stem Cell-Derived Exosomes Promotes Repair in Ischemic Myocardium. *J Cardiovasc Transl Res* 2018; **11**: 420-428 [PMID: 30232729 DOI: 10.1007/s12265-018-9822-0]

28 **Prathipati P**, Nandi SS, Mishra PK. Stem Cell-Derived Exosomes, Autophagy, Extracellular Matrix Turnover, and miRNAs in Cardiac Regeneration during Stem Cell Therapy. *Stem Cell Rev Rep* 2017; **13**: 79-91 [PMID: 27807762 DOI: 10.1007/s12015-016-9696-y]

29 **Wei W**, Ao Q, Wang X, Cao Y, Liu Y, Zheng SG, Tian X. Mesenchymal Stem Cell-Derived Exosomes: A Promising Biological Tool in Nanomedicine. *Front Pharmacol* 2020; **11**: 590470 [PMID: 33716723 DOI: 10.3389/fphar.2020.590470]

30 **Xu R**, Zhang F, Chai R, Zhou W, Hu M, Liu B, Chen X, Liu M, Xu Q, Liu N, Liu S. Exosomes derived from pro-inflammatory bone marrow-derived mesenchymal stem cells reduce inflammation and myocardial injury *via* mediating macrophage polarization. *J Cell Mol Med* 2019; **23**: 7617-7631 [PMID: 31557396 DOI: 10.1111/jcmm.14635]

31 **Ma J**, Zhao Y, Sun L, Sun X, Zhao X, Sun X, Qian H, Xu W, Zhu W. Exosomes Derived from Akt-Modified Human Umbilical Cord Mesenchymal Stem Cells Improve Cardiac Regeneration and Promote Angiogenesis *via* Activating Platelet-Derived Growth Factor D. *Stem Cells Transl Med* 2017; **6**: 51-59 [PMID: 28170176 DOI: 10.5966/sctm.2016-0038]

32 **Zhang B**, Wang M, Gong A, Zhang X, Wu X, Zhu Y, Shi H, Wu L, Zhu W, Qian H, Xu W. HucMSC-Exosome Mediated-Wnt4 Signaling Is Required for Cutaneous Wound Healing. *Stem Cells* 2015; **33**: 2158-2168 [PMID: 24964196 DOI: 10.1002/stem.1771]

33 **Chen W**, Huang Y, Han J, Yu L, Li Y, Lu Z, Li H, Liu Z, Shi C, Duan F, Xiao Y. Immunomodulatory effects of mesenchymal stromal cells-derived exosome. *Immunol Res* 2016; **64**: 831-840 [PMID: 27115513 DOI: 10.1007/s12026-016-8798-6]

34 **Cui GH**, Wu J, Mou FF, Xie WH, Wang FB, Wang QL, Fang J, Xu YW, Dong YR, Liu JR, Guo HD. Exosomes derived from hypoxia-preconditioned mesenchymal stromal cells ameliorate cognitive decline by rescuing synaptic dysfunction and regulating inflammatory responses in APP/PS1 mice. *FASEB J* 2018; **32**: 654-668 [PMID: 28970251 DOI: 10.1096/fj.201700600R]

35 **Moon GJ**, Sung JH, Kim DH, Kim EH, Cho YH, Son JP, Cha JM, Bang OY. Application of Mesenchymal Stem Cell-Derived Extracellular Vesicles for Stroke: Biodistribution and MicroRNA Study. *Transl Stroke Res* 2019; **10**: 509-521 [PMID: 30341718 DOI: 10.1007/s12975-018-0668-1]

36 **Fujii S**, Miura Y, Fujishiro A, Shindo T, Shimazu Y, Hirai H, Tahara H, Takaori-Kondo A, Ichinohe T, Maekawa T. Graft-Versus-Host Disease Amelioration by Human Bone Marrow Mesenchymal Stromal/Stem Cell-Derived Extracellular Vesicles Is Associated with Peripheral Preservation of Naive T Cell Populations. *Stem Cells* 2018; **36**: 434-445 [PMID: 29239062 DOI: 10.1002/stem.2759]

37 **Kordelas L**, Rebmann V, Ludwig AK, Radtke S, Ruesing J, Doeppner TR, Epple M, Horn PA, Beelen DW, Giebel B. MSC-derived exosomes: a novel tool to treat therapy-refractory graft-versus-host disease. *Leukemia* 2014; **28**: 970-973 [PMID: 24445866 DOI: 10.1038/leu.2014.41]

38 **Lai P**, Chen X, Guo L, Wang Y, Liu X, Liu Y, Zhou T, Huang T, Geng S, Luo C, Huang X, Wu S, Ling W, Du X, He C, Weng J. A potent immunomodulatory role of exosomes derived from mesenchymal stromal cells in preventing cGVHD. *J Hematol Oncol* 2018; **11**: 135 [PMID: 30526632 DOI: 10.1186/s13045-018-0680-7]

39 **Riazifar M**, Mohammadi MR, Pone EJ, Yeri A, Lässer C, Segaliny AI, McIntyre LL, Shelke GV, Hutchins E, Hamamoto A, Calle EN, Crescitelli R, Liao W, Pham V, Yin Y, Jayaraman J, Lakey JRT, Walsh CM, Van Keuren-Jensen K, Lotvall J, Zhao W. Stem Cell-Derived Exosomes as Nanotherapeutics for Autoimmune and Neurodegenerative Disorders. *ACS Nano* 2019; **13**: 6670-6688 [PMID: 31117376 DOI: 10.1021/acsnano.9b01004]

40 **He JG**, Li BB, Zhou L, Yan D, Xie QL, Zhao W. Indoleamine 2,3-dioxgenase-transfected mesenchymal stem cells suppress heart allograft rejection by increasing the production and activity of dendritic cells and regulatory T cells. *J Investig Med* 2020; **68**: 728-737 [PMID: 31892638 DOI: 10.1136/jim-2019-001160]

41 **He JG**, Xie QL, Li BB, Zhou L, Yan D. Exosomes Derived from IDO1-Overexpressing Rat Bone Marrow Mesenchymal Stem Cells Promote Immunotolerance of Cardiac Allografts. *Cell Transplant* 2018; **27**: 1657-1683 [PMID: 30311501 DOI: 10.1177/0963689718805375]

42 **Borghese F**, Clanchy FI. CD74: an emerging opportunity as a therapeutic target in cancer and autoimmune disease. *Expert Opin Ther Targets* 2011; **15**: 237-251 [PMID: 21208136 DOI: 10.1517/14728222.2011.550879]

43 **Schröder B**. The multifaceted roles of the invariant chain CD74--More than just a chaperone. *Biochim Biophys Acta* 2016; **1863**: 1269-1281 [PMID: 27033518 DOI: 10.1016/j.bbamcr.2016.03.026]

44 **Su H**, Na N, Zhang X, Zhao Y. The biological function and significance of CD74 in immune diseases. *Inflamm Res* 2017; **66**: 209-216 [PMID: 27752708 DOI: 10.1007/s00011-016-0995-1]

45 **Klasen C**, Ziehm T, Huber M, Asare Y, Kapurniotu A, Shachar I, Bernhagen J, El Bounkari O. LPS-mediated cell surface expression of CD74 promotes the proliferation of B cells in response to MIF. *Cell Signal* 2018; **46**: 32-42 [PMID: 29476963 DOI: 10.1016/j.cellsig.2018.02.010]

46 **Zhao S**, Molina A, Yu A, Hanson J, Cheung H, Li X, Natkunam Y. High frequency of CD74 expression in lymphomas: implications for targeted therapy using a novel anti-CD74-drug conjugate. *J Pathol Clin Res* 2019; **5**: 12-24 [PMID: 30191677 DOI: 10.1002/cjp2.114]

47 **Oeckinghaus A**, Ghosh S. The NF-kappaB family of transcription factors and its regulation. *Cold Spring Harb Perspect Biol* 2009; **1**: a000034 [PMID: 20066092 DOI: 10.1101/cshperspect.a000034]

48 **Molinero LL**, Alegre ML. Role of T cell-nuclear factor κB in transplantation. *Transplant Rev (Orlando)* 2012; **26**: 189-200 [PMID: 22074783 DOI: 10.1016/j.trre.2011.07.005]

49 **Liu B**, Korkmaz B, Kraft P, Mayer T, Sayour AA, Grundl MA, Domain R, Karck M, Szabó G, Korkmaz-Icöz S. Pharmacological inhibition of the cysteine protease cathepsin C improves graft function after heart transplantation in rats. *J Transl Med* 2023; **21**: 799 [PMID: 37946197 DOI: 10.1186/s12967-023-04659-6]

50 **Tsuji S**, Shimada S, Ono M. Modified Heterotopic Abdominal Heart Transplantation and a Novel Aortic Regurgitation Model in Rats. *J Vis Exp* 2023 [PMID: 37335093 DOI: 10.3791/64813]

51 **Matza D**, Lantner F, Bogoch Y, Flaishon L, Hershkoviz R, Shachar I. Invariant chain induces B cell maturation in a process that is independent of its chaperonic activity. *Proc Natl Acad Sci U S A* 2002; **99**: 3018-3023 [PMID: 11867743 DOI: 10.1073/pnas.052703299]

52 **Shachar I**, Flavell RA. Requirement for invariant chain in B cell maturation and function. *Science* 1996; **274**: 106-108 [PMID: 8810244 DOI: 10.1126/science.274.5284.106]

53 **Sharif O**, Bolshakov VN, Raines S, Newham P, Perkins ND. Transcriptional profiling of the LPS induced NF-kappaB response in macrophages. *BMC Immunol* 2007; **8**: 1 [PMID: 17222336 DOI: 10.1186/1471-2172-8-1]

54 **Blazquez R**, Sanchez-Margallo FM, de la Rosa O, Dalemans W, Alvarez V, Tarazona R, Casado JG. Immunomodulatory Potential of Human Adipose Mesenchymal Stem Cells Derived Exosomes on in vitro Stimulated T Cells. *Front Immunol* 2014; **5**: 556 [PMID: 25414703 DOI: 10.3389/fimmu.2014.00556]

55 **Ma ZJ**, Wang YH, Li ZG, Wang Y, Li BY, Kang HY, Wu XY. Immunosuppressive Effect of Exosomes from Mesenchymal Stromal Cells in Defined Medium on Experimental Colitis. *Int J Stem Cells* 2019; **12**: 440-448 [PMID: 31242720 DOI: 10.15283/ijsc18139]

56 **Hu W**, Song X, Yu H, Sun J, Zhao Y. Released Exosomes Contribute to the Immune Modulation of Cord Blood-Derived Stem Cells. *Front Immunol* 2020; **11**: 165 [PMID: 32161585 DOI: 10.3389/fimmu.2020.00165]

57 **Munn DH**, Mellor AL. Indoleamine 2,3 dioxygenase and metabolic control of immune responses. *Trends Immunol* 2013; **34**: 137-143 [PMID: 23103127 DOI: 10.1016/j.it.2012.10.001]

58 **Zhang H**, Dhalla NS. The Role of Pro-Inflammatory Cytokines in the Pathogenesis of Cardiovascular Disease. *Int J Mol Sci* 2024; **25** [PMID: 38256155 DOI: 10.3390/ijms25021082]

59 **Kong P**, Cui ZY, Huang XF, Zhang DD, Guo RJ, Han M. Inflammation and atherosclerosis: signaling pathways and therapeutic intervention. *Signal Transduct Target Ther* 2022; **7**: 131 [PMID: 35459215 DOI: 10.1038/s41392-022-00955-7]

60 **Tran DT**, Batchu SN, Advani A. Interferons and interferon-related pathways in heart disease. *Front Cardiovasc Med* 2024; **11**: 1357343 [PMID: 38665231 DOI: 10.3389/fcvm.2024.1357343]

61 **Liberale L**, Ministrini S, Carbone F, Camici GG, Montecucco F. Cytokines as therapeutic targets for cardio- and cerebrovascular diseases. *Basic Res Cardiol* 2021; **116**: 23 [PMID: 33770265 DOI: 10.1007/s00395-021-00863-x]

Published by **Baishideng Publishing Group Inc**
7041 Koll Center Parkway, Suite 160, Pleasanton, CA 94566, USA
Telephone: +1-925-3991568
E-mail: office@baishideng.com
Help Desk: https://www.f6publishing.com/helpdesk
https://www.wjgnet.com